Cell geometry for cluster-based quasicrystal models

Christopher L. Henley
*Department of Physics, Cornell University, Ithaca, New York, 14853-2501**
and Department of Physics, Boston University, Boston, Massachusetts 02215
(Received 14 March 1990)

A new model of the geometrical structure of icosahedral quasicrystals is discussed that is based on icosahedral clusters connected by linkages (consistent with currently accepted motifs of the atomic structure), yet that is also a tiling by four kinds of "canonical cells." Such a geometry is convenient for complete atomic structure models defined by decoration, especially if configurational disorder is to be included. The canonical-cell tiling is related and compared with previous models such as packings of Ammann rhombohedra, sphere packings on Penrose tilings, and two decoration models of Audier. The frequency of occurrence is estimated for each kind of cell or other geometrical object—the basis for stoichiometry calculations of decoration models. The 32 distinct local environments around a given cluster are described. Many useful *periodic* tilings of this class are described providing useful "rational approximants" of the true structure and hypothetical structure models for some recently discovered approximant crystal phases.

I. INTRODUCTION

In order to understand the mechanism of the formation of quasicrystals, and even more to open them up for microscopic theoretical studies of the cohesion, transport, and magnetic properties,[1,2] a good model of the atomic structure is required. There are two major classes of quasicrystals in which the basis of the order is known from examination of closely related cubic crystalline structures,[3–6] but essential details are unknown. An abundance of diffraction data has recently become available for *i*(Al-Mn-Si) (Refs. 7–10) and on *i*(Al-Cu-Li).[11,12]

There are two great difficulties in formulating a structural model for quasicrystals. One of these is that, even if the structure is perfectly quasiperiodic, the atomic positions, in principle, require an infinite number of parameters to specify. This raises practical difficulties for the fitting process. The other difficulty is the packing disorder present in most real quasicrystals.[13–15] Even *i*(Al-Cu-Fe) and *i*(Al-Cu-Ru), which have long-range translational correlations as evidenced by Bragg peaks,[16] may be realizations of a "random-tiling" model, stabilized by entropy.[17,18]

In the past two years, some progress has been made in extracting atomic positions from diffraction.[19] There are quaisperiodic tiling-like models with very reasonable local packing and stoichiometry for *i*(Al-Mn) by Duneau and Oguey[20] and for *i*(Al-Cu-Li) by Audier *et al.*[11,21,22] A serious shortcoming in the quasiperiodic-tiling-like models is their arbitariness: there is no visible implementation of the "matching rules" that would explain their quasiperiodicity.

Furthermore, atomic structures, in the form of cuts through a continuous six-dimensional density, have been derived from x-ray and neutron measurements of "Bragg" intensities.[7–10,12] The partial occupations and unrealistic local packing visible in the real-space structure[19] would be the natural effect of the ensemble averaging (implicit in neglecting diffuse scattering), if the structure is a random packing. Such disorder can be accounted for awkwardly, if at all, in either the quasiperiodic tiling or continuous density descriptions.

There is not yet any atomic structure model for any quasicrystal alloy which simultaneously (i) incorporates the packing randomness which probably occurs in real quasicrystals, (ii) has adjustable parameters which can be optimized in fits to experimental data, (iii) agrees with available diffraction information, and (iv) has chemically sensible local environments (for the composition in question).

A. Decoration models and geometrical frameworks

Decoration approaches to the structural description of quasicrystals are the most tractable. They are based on factoring the problem into parts: a "geometry" defined by (1) a set of rigid units, with (2) rules for connecting them, plus (3) rules for decorating them by atoms.

1. Objects of the geometry

A *geometry* consists of a set of *nodes* connected by *bonds*. There are just a few classes of allowed bonds; each class consists of a vector and all those equivalent to it by icosahedral symmetry; typically the bonds lie along special symmetry directions, such as the five-fold, two-fold, or three-fold symmetry axes of icosahedral symmetry. The icosahedral axes are oriented the same throughout. Depending upon the degree of order, the bonds may also form flat polygonal *faces* and these may join to form polyhedral *cells*.

Two kinds of geometry have been popular. The first kind is a "tiling." The fundamental rigid unit is taken to

be the tile (or cell), and the structure is required fill space with these objects without gaps or overlaps. In three dimensions, the cells are almost always taken to be the Ammann rhombohedra,[23,24] the cells of the three-dimensional Penrose tiling (3DPT) generated by projection.[24–27]

A second kind of geometry is a network (often called "packing") of icosahedra.[13,28,29] The fundamental rigid units are taken to be the nodes (the "icosahedra") and the linkages connecting them.

2. *Rules packing objects into geometries*

For a given set of geometric objects, it is usually possible to build structures with various kinds of long-range order (or lack thereof): periodic lattices, quasiperiodic lattices, and several kinds of random lattice, with or without long-range translational order.[30,1]

3. *Decorations*

The decoration is a rule for placing atoms in or around the objects making up the geometry. We are principally interested in *deterministic* decorations: this means that, given a geometry, there is a unique way of placing atomic sites upon it.

When attempting to formulate a decoration model, we find a conflict. On the one hand, experimental evidence suggests a packing of icosahedral clusters of two or three atomic shells both for the *i*(Al-Mn) class of quasicrystals[3,4] [which includes *i*(Al-Cu-Fe)] and the *i*(Al-Zn-Mg) class and for the *i*(Al-Zn-Mg) class[6,31] [which includes *i*(Al-Cu-Li)]. Packing such objects is the simplest way to obtain a structure possessing both strictly determined local order and also nonperiodicity (possibly randomness) at larger length scales. Yet it is difficult to formulate a decoration of such a network of icosahedra which is complete in that it also specifies the positions of the many atoms which fill the spaces between clusters.[32,33]

On the other hand, a tiling model is much more attractive technically, because space is filled by only a few kinds of objects. Then a decoration rule can place atoms in the same places in each cell of a particular class, as if it were the unit cell of a crystalline structure. Hence, a finite set of parameters suffices to specify positions for all the atoms. However, known tiling models based on Ammann rhombohedra fail to incorporate enough complete clusters. This conflict is removed in the "canonical-cell" geometry presented in this paper, which is both tiling and network of icosahedra.

B. Outline of the paper

This paper is the first of two intended to present a different way to set up a complete and realistic structural model of the atomic structure. By "complete," I mean that the atomic decoration has a one-to-one relationship to the geometry and accounts for all the atoms. By "realistic," I mean the model should conform to everything known about the local arrangements in the alloy being modeled, and in related crystalline structures. This paper focuses on the geometry; a subsequent one[34] will describe model decorations and discuss how much information about them may be extracted from diffraction data.

Previous work suggests that a realistic geometry should be some sort of network of icosahedral clusters with linkages in two-fold and three-fold directions (a broad class including many kinds of ordered and random structures). Restrictions are added to this model to make it into a new kind of tiling with four kinds of *canonical cells*; these structures are explored in the remainder of the paper. Section II defines the elements of the canonical-cell geometry and the rules for packing the cells together. To connect to previous decoration models,[4,3,6] it is shown how a canonical cell packing can be turned into a tiling of (smaller) Ammann polyhedra. Section III presents notations and relations useful for analyzing and comparing canonical-cell tilings by the frequencies of local patterns. It is shown that there is only one degree of freedom [parametrized by ζ, see Eqs. (3.6)] which specifies the volume occupied by different types of cell and the packing fraction. Furthermore, a nomenclature is given for naming, and a scheme found for enumerating, the 32 allowed environments of nodes in the network.

Section IV shows how structures periodic in one or more directions can be constructed from canonical cells. Such "approximant" models are important because (i) many approximant crystals closely related to quasicrystals have recently been discovered in nature,[22,35–37] and (ii) atomic models which approximate the nonperiodic icosahedral structure, yet satisfy periodic boundary conditions, are more practical technically in many theoretical calculations. To conclude, Sec. V discusses applications of the results, recent elaborations in cluster-packing models, and the difficulties in producing infinite canonical-cell structures.

In addition, there are four appendices. An arbitrary tiling can be viewed as a projection from a higher-dimensional space, where it forms a continuous faceted (hyper)surface which can be usefully treated in a coarse-grained fashion;[1,25] Appendix A reviews applications of this description that are used in this paper. Appendices B and C discuss two ways in which Penrose tilings can be decorated to produce perfectly quasiperiodic networks of icosahedra closely related to canonical cells, and why these constructions are inadequate. Appendix D reports the methods used for the complete enumeration of vertex types.

II. RULES FOR CANONICAL-CELL PACKINGS

This section motivates (Sec. II A) and defines (Sec. II B) the four kinds of canonical cells and their packing rules used in the rest of this paper. The most significant property of canonical-cell packings is that they are both tilings and cluster networks; this allows them to satisfy the criteria of Sec. II A for geometries allowing well-formulated decorations even in random structures. They are compared (in Sec. II A) to previous cluster packings, inadequate by these criteria, and (in Sec. II C) are related to previous tilings using Ammann rhombohedra.

A. Principles for networks of icosahedra

Let us start with the fairly standard picture of a network of icosahedral nodes[3,4] joined by "linkages" which are perfectly rigid in length and perfectly oriented along twofold or threefold icosahedral directions. Two kinds of nearest-neighbor linkage are allowed, called "b," in the twofold direction and "c," in the threefold direction [Fig. 1(a)]. These names will also be used for their lengths. We will use b as the unit of length, related to the usual "quasilattice constant" (rhombohedron edge length)[25] by

$$b \equiv 2(\tau^3/\sqrt{5})^{1/2} a_R \tag{2.1}$$

and then

$$c \equiv (\sqrt{3}/2) b \ . \tag{2.2}$$

In order to get the correct space group, the c linkage suffices[13,38] but to get a well connected network, we need the twofold (b) linkage.[28,39,40]

It will also be assumed that nearby nodes are only related by displacements of these allowed types (this excludes the wall defects known as "tears"[28] characteristic of the more disordered packing models[13,29]). The linkages of the network *may*, but need not, define faces which *may* enclose cells.

1. Desired features for decoration models

Decorations for a geometry are rules which, given any realization that satisfies the packing rules, produces a set of atomic sites. The obvious decoration for a packing of icosahedra is to placing identical clusters of atoms on each node. In this case, the Fourier transform of the scattering density would simply be a product of the geometrical structure factor of the centers times a form factor for the cluster.[41,42] In reality, other atoms (identified as "glue" atoms) must be placed at sites in the interstices between clusters. Structural modeling starting from random cluster packings has been awkward; there is a great variety of different kinds of interstices, some quite large, so a straight forward rule is impossible. Instead, a procedure may define candidate sites in rings around each cluster, and then use a heuristic rule to eliminate conflicting sites.[32,33]

We escape these problems by satisfying the following.

Criterion C0: The geometry is a tiling (no overlaps or gaps), and there is a unique way of decorating each object.[43] Such a rule is obviously *deterministic*, i.e., each realization of the geometry corresponds to a *unique* realization of the decoration).[44] Also, since there is a finite set of objects, there is a finite set of rules. Some corollaries of ($C0$) are the following.

Corollary C0-1: The Fourier transform of the atomic structure is a sum of products of form factors and geometrical structure factors.[42]

Corollary C0-2: The symmetry of an object's decoration is the intersection of the object's symmetry[45] and the icosahedral point group $\bar{5}\,\bar{3}2/m$. For the case of the canonical-cell tiling, these symmetries are listed in Table I.

Corollary C0-3: The atomic structure has the same space group as the geometry.

2. Desired features for the geometry

Physical intuition suggests the following criteria for a good geometry.

Criterion C1: We presume the compositions at which icosahedral phases form are those where the chemistry most favors the presence of icosahedral clusters in the structure; therefore, we demand that the fraction of all atoms that belong to such clusters be as large as possible. Since the overall density of atoms is essentially fixed, this means the *number density* of clusters, or equivalently the *packing fraction* of clusters (considered as spheres), must be as large as possible.

Criterion C2: To develop long-range orientational order as in the icosahedral phase, the clusters must be packed in a way that strongly favors having the same orientation. Furthermore, the energetics must strongly favor neighboring clusters having as many linkages as possible; if they did not, the defects that disrupt the translational order would have high densities contrary to observation. Hence, we demand that the network have *as high a coordination number* as possible. (Of course, if the coordination number is high, the density must be high also.)

Criterion C3: If the clusters are well packed, the interstices between are relatively small and most of the "glue" atoms that fill these spaces will be in contact with atoms of the surrounding clusters. Also, if the "linkages" are strongly favored, this suggests there are special arrangements of atoms associated with them.[4] So, physically, we expect that the "glue" atoms are fairly well ordered and it follows that the set of favored shapes for interstices in the network geometry is relatively limited. Furthermore, a tractable model cannot have too many decoration rules. Hence, we also demand that the structure have *as few types of cells as possible* (corresponding to the interstices of the network).

A model geometry based on the "twelvefold" sites, a decoration of the ideal 3D Penrose tiling, was developed but is deficient by the above criteria. Namely, (i) the packing fraction (density of nodes) is too low (see Table III, later), (ii) the coordination numbers are also too small, and (iii) there are too many different kinds of interstices—some rather big, yet too small to fit an additional cluster. Data on this model are given in Ref. 46 and in Appendix B. Two recent structural models, by Duneau and Oguey[20,47] and by Yamamoto and Hiraga,[48] have proceeded by using cut-and-project to define a subset of Penrose tiling vertices to place clusters (a "sphere packing"). The quasiperiodic network of clusters used, however, is essentially identical to the "twelvefold packing."[46] A different decoration, due to Audier and Guyot,[38,49] produces a similar geometry with similar deficiencies (see Appendix C). Models generated by random growth processes, with carefully adjusted annealing,[28] can do better but still have many kinds of local holes in the network, the decoration of which is hard to specify.

B. Canonical cells

All the criteria can be met if we restrict not only the types of possible linkages, but the types of possible inter-

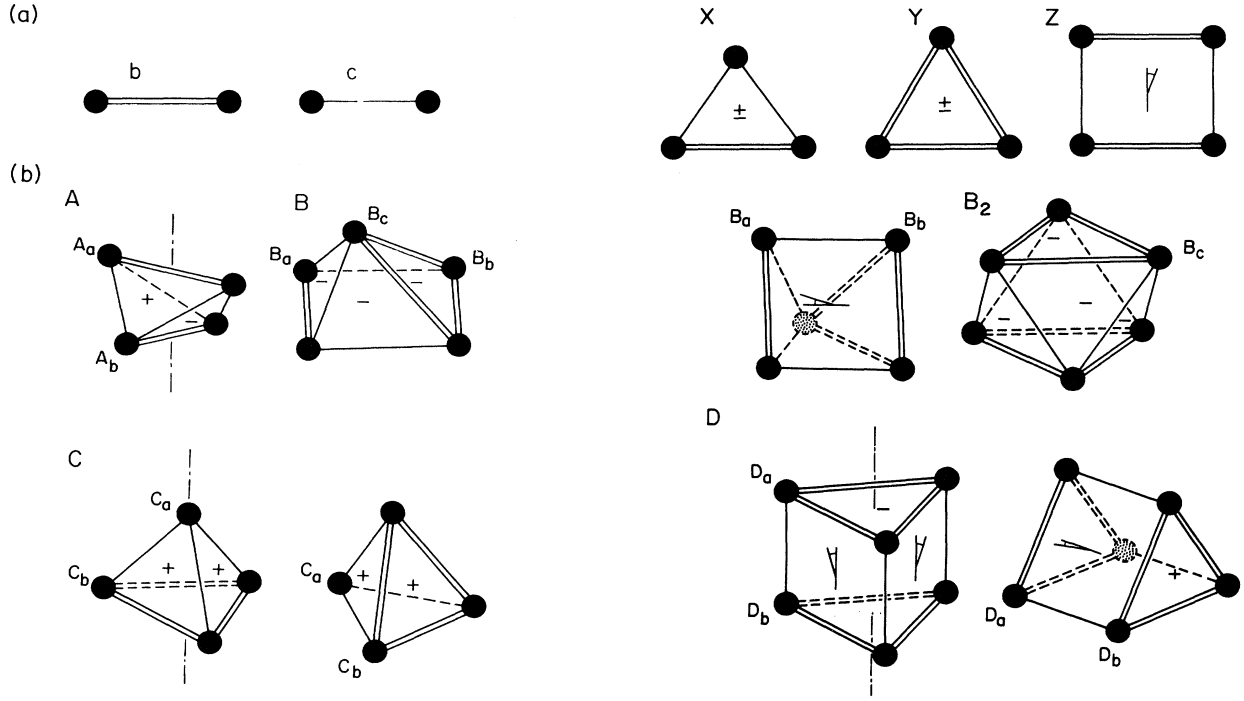

FIG. 1. (a) Canonical bonds (b,c) and faces (X,Y,Z). Nodes are always shown by solid circles (dashed and stippled if hidden). Markings on the faces are the abstract decorations which implement the packing rules which ensure the cells are oriented correctly with respect to the icosahedral axes. (b) Canonical cells A, B, C, and D. Two views each are shown for the B, C, and D cells. The different corner types are labeled. The B_2 unit, also shown, may be divided into two B cells by cutting along any one of its three internal rectangles.

stitial cells and faces shall be limited to a short list of "canonical" cells and faces. The resulting structure is thus a tiling. The name "canonical cells" is chosen by analogy with the "canonical holes," which were classified by Bernal.[50] These were the interstices in random close packings of spheres modeling the structure of amorphous alloys. The rest of this paper develops a tiling based on four canonical cells.

The allowed linkages and the three kinds of allowed faces are shown in Fig. 1(a). The canonical faces are an isosceles triangle ("X"), an equilaterial triangle ("Y"), and a rectangle ("Z").

TABLE I. Geometrical objects of canonical-cell tiling.

Symbol	identification	Symmetry	[apparent symm.][a]	Measure
	Node	$\bar{5}\bar{3}m$	[full]	
b	Twofold bond	$2/mm$	$[\infty/mm]$	b
c	Threefold bond	$\bar{3}m$	$[\infty/mm]$	$\frac{\sqrt{3}}{2}b$
X	Isosceles triangle	$2m$	$[2/mm]$	$\frac{1}{2\sqrt{2}}b^2$
Y	Equilateral triangle	$3m$	$[3/mm]$	$\frac{\sqrt{3}}{4}b^2$
Z	Rectangle	$2/m$	$[2/mm]$	$\frac{\sqrt{3}}{2}b^2$
A	bcc tetrahedron	$2m$	$[\bar{4}m]$	$\frac{1}{12}b^3\cong 0.083b^3$
B	Pyramid	m		$\frac{\sqrt{5}}{12}b^3\cong 0.186b^3$
B_2	"Octahedron"	$\bar{3}m$		$\frac{\sqrt{5}}{6}b^3\cong 0.373b^3$
C	(Triang.) tetrahedron	$3m$		$\frac{\sqrt{5}}{24}b^3\cong 0.093b^3$
D	Trigonal prism	$3m$	$[\bar{3}/mm]$	$\frac{3}{8}b^3\cong 0.375b^3$

[a]Brackets indicate apparent symmetry of the cell's outline; when the decorations are considered, the lower symmetry is correct.

The four kinds of cells allowed[51] are shown in Fig. 1(b). They may be understood best by noting that each kind can be packed into a simple periodic structure. The *A* cell ("bcc tetrahedron"), is a tetrahedron with two twofold linkages perpendicular; these pack together to form a bcc "*A*" structure, which describes the α(Al-Mn-Si) phase. The *B* cell is half of a triangular antiprism which is a slightly distorted octahedron; it will often be useful to consider the trigonal antiprism (a flattened "octahedron") B_2 by itself since it has greater symmetry (threefold axis). The *C* cell is a triangular pyramid, somewhat flattened compared to a regular tetrahedron. The *B* and *C* cells pack to form a rhomboheral "*BC*" structure which is an fcc packing compressed (along the threefold axis) by a factor $\sqrt{5/8}$. Finally, the *D* cell is a trigonal prism and it packs into a trigonal "*D*" structure.

It is important to note that the objects have less symmetry than they appear to.[52] For example, an equilateral triangle has point symmetry group $3/mm$, which includes a mirror reflection in the triangle's plane. However, the icosahedral group does not contain such a mirror operation, so when we consider the atoms, the two sides of the face are not equivalent. The same thing happens wih the isosceles triangle. We will indicate this by marking the two sides of each triangular face with + and − signs (see Fig. 1). In general, the actual symmetry of an

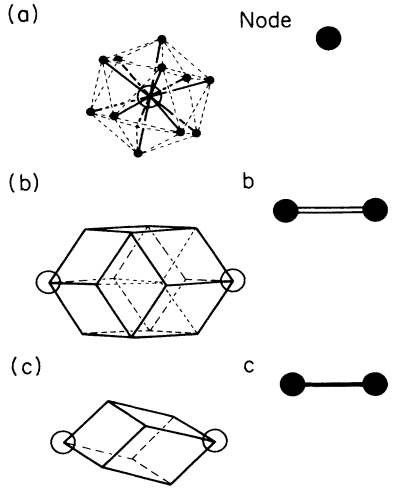

FIG. 2. Relation of canonical bonds to rhombohedral decoration. The node and bonds on the right correspond to the rhombohedral groupings on the left. (a) Each node becomes a vertex (open circle) in the rhombohedral tiling with edges (heavy solid lines) radiating in all 12 possible directions. The neighboring vertices (small solid circles) form an icosahedron. (b) Each twofold (*b*) bond becomes a rhombic dodecahedron (RD). The dotted lines show one of the two ways of breaking it into two prolate and two oblate rhombohedra. (c) Each *c* bond becomes a prolate rhombohedron.

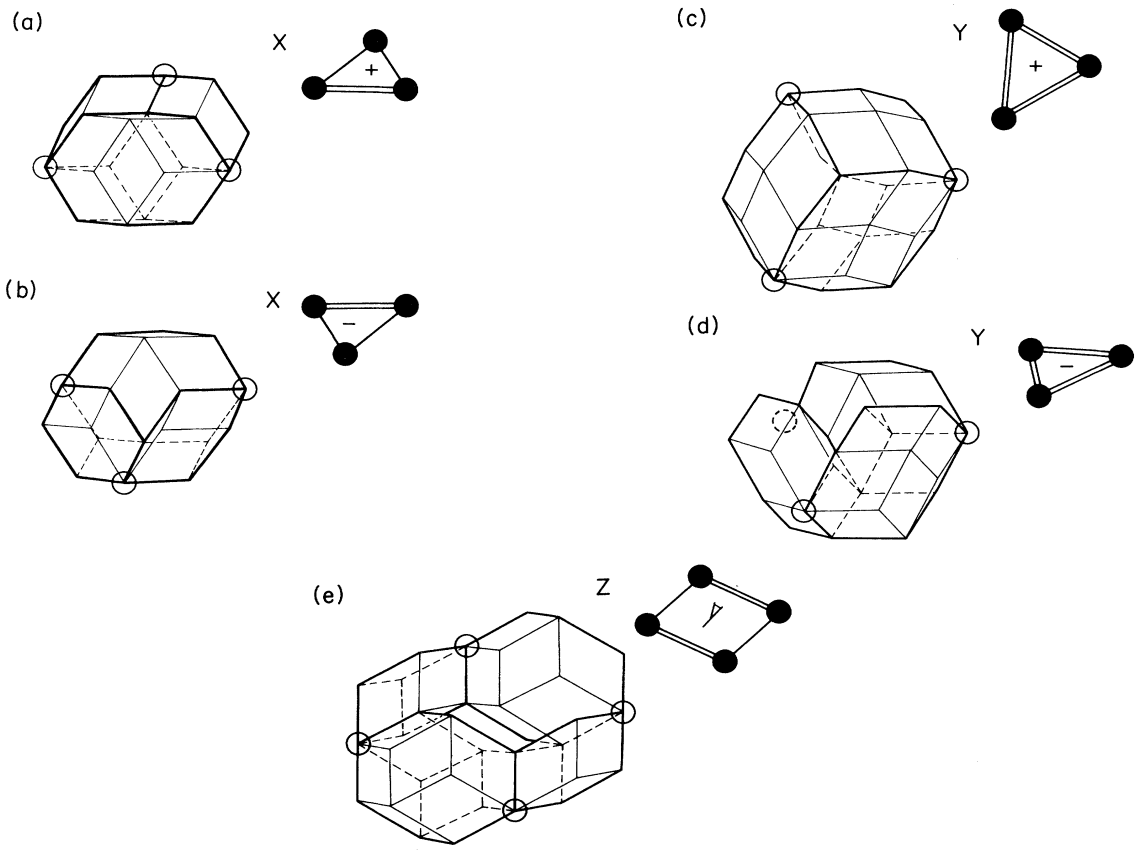

FIG. 3. Bonds on cell faces and rhombohedral decoration. The *X* faces [(a) and (b)] and *Y* faces [(c) and (d)] are shown from both sides; the *Z* face (d) has both sides equivalent. The RD and PR decorating *b* and *c* bonds are outlined with heavy lines. One some of the nearer RD and PR tiles, hidden edges are shown dashed.

TABLE II. Contents of canonical cells.

Cell	Nodes	Bonds		Volume	Rhombohedra Prolate	Rhombohedra Oblate
A	1/6	1/2	2/3	$\frac{1}{3}\tau^4 V_P = \frac{1}{12}b^3$	5/3	1
$B+C$	1/2	3/2	3/2	$\frac{1}{2}\sqrt{5}\tau^4 V_P = \frac{\sqrt{5}}{8}b^3$	11/2	7/2
D	1/2	3/2	1/2	$\frac{3}{2}\tau^4 V_P = \frac{3}{8}b^3$	15/2	9/2

object is the intersection of the apparent symmetry of the outline of the edges and the icosahedral group $\bar{5}\bar{3}2/m$. The volumes and symmetries of the canonical objects are given in Table I. Other information about the canonical cells and their corners is given in Table II. (V_P is the volume of the prolate rhombohedron.) Notice how the number of nodes per cell can be defined by allotting fractional nodes proportional to the part of surrounding solid angle belonging to the cell.

Thus, when the cells pack together, we enforce a constrained packing rule that the + and − signs (see Fig. 1) must match: if the outside face on one cell is +, the outside face of the adjoining one must be −. This is exactly the sort of restriction imposed by "matching rules," but the constrained packing rules do not suffice to specify the structure the way "strong" matching rules do (up to local isomorphism class) for ideal quasiperiodic tilings.[53,54]

C. Rhombohedral decoration and packing

Here a "standard" decoration of the canonical cells is described that turns any packing of canonical cells into a packing of tiles called prolate rhombohedron (PR), oblate rhombohedron (OR), and rhombic dodecahedron (RD) (to reduce confusion, the term "tile" will be reserved for these units, although canonical cells are, of course, tiles too). The PR and OR are the Ammann rhombohedra of the 3D Penrose tiling projected from a 6D hypercubic lattice, which has been used by many authors as the geometry for decoration models. The rhombohedron edges run along five-fold symmetry axes and have length a_R related to b by Eq. (2.1). (In real materials, $a_R \approx 5$ Å). The RD is a packing of two PR and two OR which are welded together to form a polyhedron of greater symmetry (mmm). An earlier version of the atomic decoration[4,6] was based on the OR, PR, and RD; the RD needed to be treated as a distinct tiling unit with its own decoration. (Later, when we count the contents of a cell in rhombohedra, the RD will count as if redivided into 2 PR + 2 OR.) The constraints of consistency with this earlier work are enough to determine the rhombohedral decoration completely.

There is a double motivation to study this decomposition: (a) To help visualize the canonical cell structures. (b) To systematically compare decorations based on canonical cells with those based on rhombohedra. (In particular, the latter can be used as a hint in generating the former.[34])

Specification of rhombohedral decoration: For every c linkage, we place a PR connecting the two tips, and similarly for every b linkage we place an RD [Fig. 2(b)], as was already done in Refs. 4 and 6. Figure 3 shows how these rhombohedra appear on the canonical faces. The correspondence of the abstract decoration and the rhombohedral decoration is also indicated (for both sides of a face, if they are inequivalent).

In the A cell, the two RD from b linkages fill the interior completely, with the top face of one fitting against the side face of the other [exactly as illustrated in Ref. 4, since the α(Al-Mn-Si) geometry is a packing of A cells]. All other cells produce additional rhombohedra which are not associated with bonds. In the most economial description, there are three kinds of extra rhombohedra (Fig. 4):

(a) Each Y face (equilateral triangle) has a PR piercing it along its threefold axis [Fig. 4(a)]. The hole into which this is inserted is obvious in Fig. 3(d). Around it, there are always three PR's (not shown) which have lower endpoints at nodes defining the Y face, share the upper faces of the central PR, and share with it their upper end-

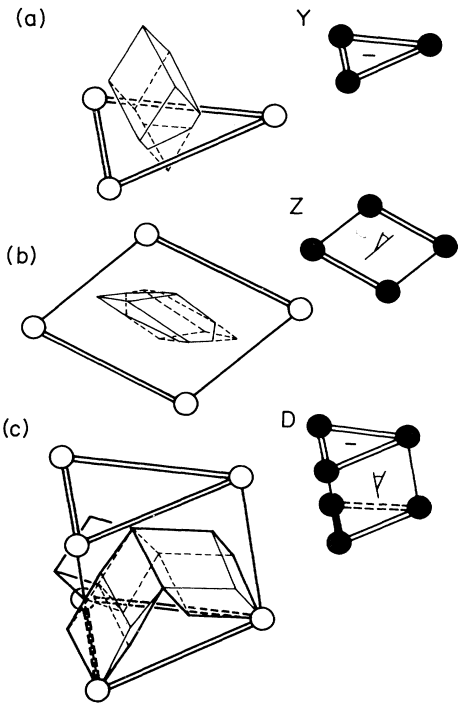

FIG. 4. Extra rhombohedra in the rhombohedral decoration. The gaps left after the bonds are decorated as in Figs. 2 and 3 are filled by (a) a PR sticking through each Y face, (b) an OR tilted through each Z face, and (c) three PR's in each D cell.

points. In the case of the C cell, the three PR's decorate c bonds and their common upper vertex is the node at the apex; in the case of the D cell, they are the PR's shown in Fig. 4(c) and their common vertex is the bottom tip of another PR through the upper Y face.

(b) Each rectangular (Z) face divides a tilted OR in half [Fig. 4(b)] with the stub through the Z along the threefold axis of the OR. [The thin hole where the OR fits is obvious in Fig. 3(e).] Note that if we break up B_2 into $B+B$ (which can be done in three equivalent ways), its internal OR becomes the OR decorating a Z face; then the OR of Fig. 4(b) is symmetrically oriented at the center of the B_2 cell with its own threefold axis coinciding with that of the B_2. However, in the B_2 cell (not shown in Fig. 4), a hole is left inside which is exactly filled by an OR.

(c) There are still left over the three PR connected to vertices in the D cell, which must be associated with its interior rather than its faces [Fig. 4(c)]. Sharing the inside faces of these three is the PR decorating the bottom Y face, and around their upper outside faces are the three OR associated with (and bisected by) the rectangular Z faces.

To summarize, we have exhibited a decoration by PR, OR, and RD rhombohedral tiles, of the linkages, faces, or cell interiors of the canonical-cell structure. There are five categories of decorating objects: the RD and PR associated with linkages b and c, the RD associated with the Y face, the OR associated with the Z face, and the PR's associated with the D cell. This decoration enforces exactly the same constrained packing rules for the cells as the abstract decoration of Sec. II B in terms of "±" signs and stubs.[55]

III. STATISTICAL DESCRIPTION OF CANONICAL-CELL TILINGS

Apart from the diffraction pattern, one of the main predictions we expect of a decoration model is the stoichiometry, and the frequency of various local environments (e.g., how many of the Mn atoms occur in pairs). In a quasiperiodic structure generated by cut-and-projection, one can calculate these directly by evaluating the volume of the intersection of various translates of the acceptance volumes in the "perpendicular space."[46] However, one motivation for developing the canonical-cell geometry is its use in formulating a random-tiling model, and the perpendicular space approach is useless for local correlations in random tilings.

This section lays the basis for describing the stoichiometry and local environments in canonical-cell structures. Section III A derives constraints on the number frequencies of the different geometrical objects. Given icosahedral symmetry, one parameter describes the possible concentrations of the four kinds of cells, instead of the three degrees of freedom we would naively expect. Furthermore, from existing information one can guess which values are most reasonable for this parameter. Then we can verify that the packing fraction in a canonical-cell packing is better than in the quasiperiodic icosahedral cluster packing.

Complicated structures are usefully characterized by the statistical distribution of the many possible local environments; Sec. III B explains how to construct pictures (as two-dimensional tilings of the unit sphere) and labels for the environments. From the packing rules on the unit sphere, induced by the 3D cell-packing rules, the complete list of possible local environments is found.

Section III C derives forcing rules which allow quick recognition of forbidden and allowed arrangements (useful when growing structures). The forcing rules eliminate so many possibilities that we can finish the enumeration of all local environments by pure brute-force reasoning, case by case. The most striking result is how few environments there are, an indication that the canonical-cell rules are quite restrictive. Besides a natural sequel of the similar study of the "twelvefold packing" (see Appendix B and Ref. 46), it is a useful way to compare different geometries based on these linkages (e.g., see Ref. 28). Furthermore, it is one piece of the vocabulary for describing particular periodic structures in Sec. IV.

A. Sum rules and frequencies of objects

The simplest kind of information we can have about a canonical-cell packing is the volume density of cells of the different types. These densities will be written $n(A), n(B), \ldots$. Since each cell will have a unique decoration by atoms,[34] the frequencies of cells will give the stoichiometry and mass density. In this part we determine some geometrical constraints on the frequencies.

1. Pairing of B and C cells

According to the matching rule for triangular Y faces, each such face must belong on one side to a cell in which the face has an outward directed arrow and on the other side must belong to a cell in which the face has an inward directed arrow. Now, the B cell has one outward arrow, the C cell has one inward arrow, and the D cell has one of each. Therefore, $n(B)=n(C)$, which must be satisfied in *any* unbounded packing of canonical cells.[56] From now on, we will write

$$n(BC)\equiv n(B)=n(C)\ . \tag{3.1}$$

2. Fraction of BC cells

In tilings of rhombi or rhombohedra, there are simple formulas for the number density of each kind of cell, in each possible orientation, as a function of the "phason strain" tensor A.[57] The meaning of "phason strain" is discussed in Appendix A. Briefly, (i) a structure of icosahedral symmetry must have zero phason strain, (ii) a random tiling (see also Sec. V) includes random phason strains, but at large scales the phason strain should average out to zero in any realization,[1,28,58,59] and (iii) periodic or layered structures made of the same units, called "approximants" (see Sec. IV) are special, commensurately locked cases of the canonical-cell structures with special uniform, nonzero values of phason strain.

In the case of the canonical-cell tilings, we can decompose each canonical cell into Ammann rhombohedra (PR and OR) as described in Sec. II C. The densities of these rhombohedra, in each orientation, are given by the same functions of the phason strain as in any other packing of the Ammann rhombohedra. Thus, 20 liner equations for the densities of the canonical cells are obtained. Unfortunately, there are many more unknowns than equations. For, grouping together the orientations related by an inversion (these have the same content of rhombohedra, since rhombohedra are invariant under inversion), we still find 10 orientations each for B_2, C, and D cells, and 15 orientations for A cells, or a total of 45 unknowns.

Happily, we can salvage one simple, useful equation by grouping together *all* the orientations. The numbers of PR and OR in each canonical cell are given in Table II. Thus,

$$n(\mathrm{PR})=\tfrac{5}{3}n(A)+\tfrac{11}{2}n(BC)+\tfrac{15}{2}n(D) \tag{3.2a}$$

and

$$n(\mathrm{OR})=n(A)+\tfrac{7}{2}n(BC)+\tfrac{9}{2}n(D) \tag{3.2b}$$

(which is still true even without icosahedral symmetry).

From Appendix A, Eq. (A4), we find for the rhombohedron densities[60]

$$n(\mathrm{PR})/n(\mathrm{OR})=(\tau-\det\mathsf{A})/(1+\tau\det\mathsf{A}) , \tag{3.3}$$

where the determinant $\det\mathsf{A}=0$ if we have icosahedral symmetry. Substituting (3.3) into (3.2), we finally get

$$n(A)+\tfrac{9}{2}n(D)=\tfrac{3}{2}\sqrt{5}\left[\frac{1-\tau^9\det\mathsf{A}}{1+\tau^9\det\mathsf{A}}\right]n(BC) . \tag{3.4}$$

We now have two nontrivial linear equations (3.1) and (3.4) in $n(A),n(B),\ldots$ as well as the more trivial one from the constraint that the cells exactly fill space.

Let us define μ as the volume fraction occupied by A and D cells. Combining (3.4) with the volumes given in Table II, we see that

$$\mu=\tfrac{1}{2}(1-\tau^9\det\mathsf{A}) . \tag{3.5}$$

So, in the case of icosahedral symmetry, exactly half the volume is occupied by AD cells and exactly half by BC cells. The nontrivial parameter, which apparently is *not* determined by the phason strain, is ζ defined by letting $\mu\zeta$ be the volume fraction occupied by D cells, so that ζ measures the relative importance of D cells. Then

$$n(A)=12\mu(1-\zeta)/b^3 , \tag{3.6a}$$

$$n(BC)=(8/\sqrt{5})(1-\mu)/b^3 , \tag{3.6b}$$

$$n(D)=(8/3)\mu\zeta/b^3 . \tag{3.6c}$$

3. *Coordination number and packing fraction*

The average coordination number is obviously

$$\bar{Z}=\bar{Z}_b+\bar{Z}_c\equiv 2[n(b)+n(c)]/n , \tag{3.7}$$

where $n(b)$ and $n(c)$ are the densities of b and c linkages, and n is the total number of nodes. Combining (3.6), (3.7), and the fractional contents of nodes and linkages in cells from Table II, we find densities

$$n(b)=\left[\frac{12}{\sqrt{5}}(1-\mu)+6\mu-2\mu\zeta\right]\Big/b^3 , \tag{3.8a}$$

$$n(c)=\left[\frac{12}{\sqrt{5}}(1-\mu)+8\mu-\tfrac{20}{3}\mu\zeta\right]\Big/b^3 , \tag{3.8b}$$

$$n=\tfrac{1}{3}n(b) . \tag{3.8c}$$

Thus, in particular,

$$\bar{Z}_b=6 , \tag{3.9}$$

an identity valid in *any* unbounded canonical-cell structure. Also, for the case of icosahedral symmetry ($\mu\equiv\frac{1}{2}$), Eq. (3.8) gives

$$\begin{aligned}\bar{Z}&=4[(36+21\sqrt{5})-13\sqrt{5}\zeta]/[(6+3\sqrt{5})-\sqrt{5}\zeta]\\&=13.056(1-0.350\zeta)/(1-0.176\zeta) .\end{aligned} \tag{3.10}$$

The packing fraction f is defined by replacing the node with identical spheres with the largest possible diameter, that is c, so each has a volume $\pi c^3/6$ and (for $\mu\equiv\frac{1}{2}$)

$$f=(\pi c^3/6)n\approx 0.6442-0.1134\zeta . \tag{3.11}$$

4. *Expected values of packing fraction and D-cell fraction*

We are interested in the value of ζ in infinite icosahedral structures. No infinite model has yet been constructed (see Sec. V A), but we can use large approximants (see Table VII) to guess the value $\zeta\approx 0.3$ in the limit of icosahedral symmetry. Alternatively, we can match to previously studied icoshedral networks using the same b and c linkages, but without "canonical" rules. In the twelvefold network (Appendix B), we can count node combinations in the form of canonical cells (these are not quite cells since they can overlap); the *ratio* between A- and D-cell densities then corresponds to $\zeta\approx 0.189$. In Elser's annealed growth model,[28] which (see Sec. VI B 1) closely approximates canonical cells, we get $(\bar{Z}_b,\bar{Z}_c)=(5.86,6.25)$ for the best value (0.001) of his reduced growth velocity; matching the ratio $\bar{Z}_c/\bar{Z}_c$ gives $\zeta\approx 0.28$, while his packing fraction $f=0.615$ would give $\zeta\le 0.23$ (the inequality allows for a small density of noncanonical holes).

The above considerations lead one to expect ζ to be 0.2 or 0.3. Consistent with this, analysis of an extended x-ray-absorption fine-structure (EXAFS) experiment[61,62] gave $\bar{Z}_c\approx 6.6$ (b linkages were not considered), which corresponds to $\zeta=0.2$. The packing fractions and coordinations for icosahedrally symmetric canonical-cell packings are shown in Table III as a function of ζ. The best packing in any canonical-cell structure is $f=\sqrt{3}\pi/8\cong 0.680$, $\bar{Z}=14$, in the 1/1 (bcc) network. On the other hand, "random close packing"[63] has packing fraction $f_{\mathrm{rcp}}\approx 0.64$; according to Nelson,[64] with an ideal coordination number $\bar{Z}_{\mathrm{rcp}}\approx 13.397$ within Coxeter's "random-froth" approximation.

TABLE III. Coordination and packing fraction in various structures.

Packing	ζ	$\bar{Z}_b$	$\bar{Z}_c$	$\bar{Z}$	f
Periodic					
1/1 cubic	0	6	8	14	0.6802
2/1 cubic	0	6	7	13	0.6423
BC		6	6	12	0.6084
D	1.00	6	2	8	0.4534
3/2 cubic	0.333	6	6.25	12.25	0.6065
"Twelvefold" packing[a,b]	0.19[c]	5.825	5.528	11.353	0.5535
Annealed random aggregation[b,d]	0.28(?)	5.86	6.25	12.1	0.615±0.003
Canonical-cell packings[e]	0	6	7.056	13.056	0.6442
	0.10	6	6.824	12.824	0.6329
	0.20	6	6.584	12.584	0.6215
	0.30	6	6.334	12.334	0.6102
	0.50	6	5.807	11.807	0.5875
	1.0	6	4.292	10.292	0.5308

[a]Reference 46.
[b]In these structures, canonical cells do not fill space.
[c]From the ratio of *A* and *D* cells (see Appendix B).
[d]Reference 28.
[e]Assuming statistical icosahedral symmetry.

B. Classification of node environments

Counting the frequencies of different node types is a compact way to characterize different geometries. Furthermore, in a decoration model, the node and cell frequencies directly give the frequencies of different *atom* environments.

As with the 3D Penrose tiling,[46] nodes may be classified by either (i) the arrangement of cell solid angles packed around the node, or else, (ii) the arrangement of linkages which converge at the node. These descriptions are equivalent: given either, we could generate the other.

1. Scheme for depicting node environments

It is convenient to represent each node's surroundings by projecting the neighboring nodes and cell faces onto a unit sphere imagined to surround the node.[46] This is then represented two-dimensionally by a sort of projection, where the projection of a reference icosahedron is also shown as a sort of coordinate system (see Figs. 5–7).

This is a *tiling* of the reference sphere by two-dimensional tiles. First, there are two types of vertices: projections of *b* and *c* linkages, depicted by crosses and triangles, respectively [Fig. 5(a)].

Secondly, there are four kinds of edges of the 2D spherical tiles, projections at the node of the corners of canonical-cell faces [Fig. 5(b)]. Here *b* and *c* linkages between the neighboring nodes are represented by double and single lines, respectively. Finally, there are nine types of 2D "tiles," spherical polygons projected down from the solid corners of canonical cells, as in Fig. 5(c). Each canonical cell has two crystallographically distinct types of corners, as indicated (A_a, etc.) in Fig. 1. The *B* cell also has a corner B_c which is equivalent to a combination of a B_a and a B_b corner. The decorations which enforce the 3D face-packing rules (Sec. II B) induce 2D spherical edge-packing rules. The latter are shown in Fig. 5(b), which also indicates the types of 2D spherical "tiles" allowed on each side of each 2D spherical "edge."

This pictorial code is also intended to suggest how the vertex appears when the cell packing is translated into the language of the rhombohedral decoration (Sec. II C). Each end of a *b* linkage becomes a rhombic dodecahedron tip that fills two triangles of the reference icosahedron; each end of a *c* linkage makes a prolate rhombohedron tip that fills one triangle. Reviewing Fig. 5, it is evident that, in a canonical-cell node environment, the *only* unfilled icosahedron triangles are in the middle of C_a and D_b projected corners. These correspond, respectively, to the tip of the extra prolate rhombohedra from the opposite *Y* face in the *C* cell [Fig. 4(a)], and to the D_b corner in the *D* cell [Fig. 4(c)].

The corner angles and the areas of the spherical polygons marked in Fig. 5(c) are, of course, the same as (respectively) the angles between faces along the edge of the canonical cell, and the solid angles of the cell corners $\Omega(A_a), \ldots$. Here

$$\epsilon \equiv \cos^{-1}(\tfrac{1}{4}) \approx 4\pi(0.1049)$$

and

$$\eta \equiv \cos^{-1}(1/\sqrt{6}) \approx 4\pi(0.0915) .$$

(Recall that, by spherical trigonometry, the area of each spherical polygon is the angular excess in the sum of the corner angles.) Table IV shows the contents of each canonical cell when nodes and linkages are apportioned according to the solid angles at canonical-cell corners and edges.

2. *Nomenclature for node environments*

For practical work with models, it should be easy to find the name of a given environment, and obviously the name should be invariant under rotations. (To construct the environment given the name, one can always use a table.[65]) In 3D, it is simplest to base the label on counts of selected features within the environment. The labeling will be based on

$$(\beta,\gamma)=(N(b),N(c)) ,$$

the number of b and c linkages at that node [note $(\bar{\beta},\bar{\gamma})\equiv(\bar{Z}_b,\bar{Z}_c)$ in Eq. (3.7)]. To fully distinguish node types, we look at each fivefold direction and look at the pentagon of edges surrounding it. Any b linkage centered on one of those edges fills a polygon of two triangles, with a acute tip at the five-fold direction. Let p be the total number of such linkages around the fivefold direction (it is easy to read off from the above-described diagrams). In the twelve-fold packing,[46] this scheme was used and it sufficed to write $(\beta,\gamma)_P$, appending P, the largest p value over all fivefold directions. For the canonical-cell tiling this does not suffice: for example, one can construct three distinct environments by rotating

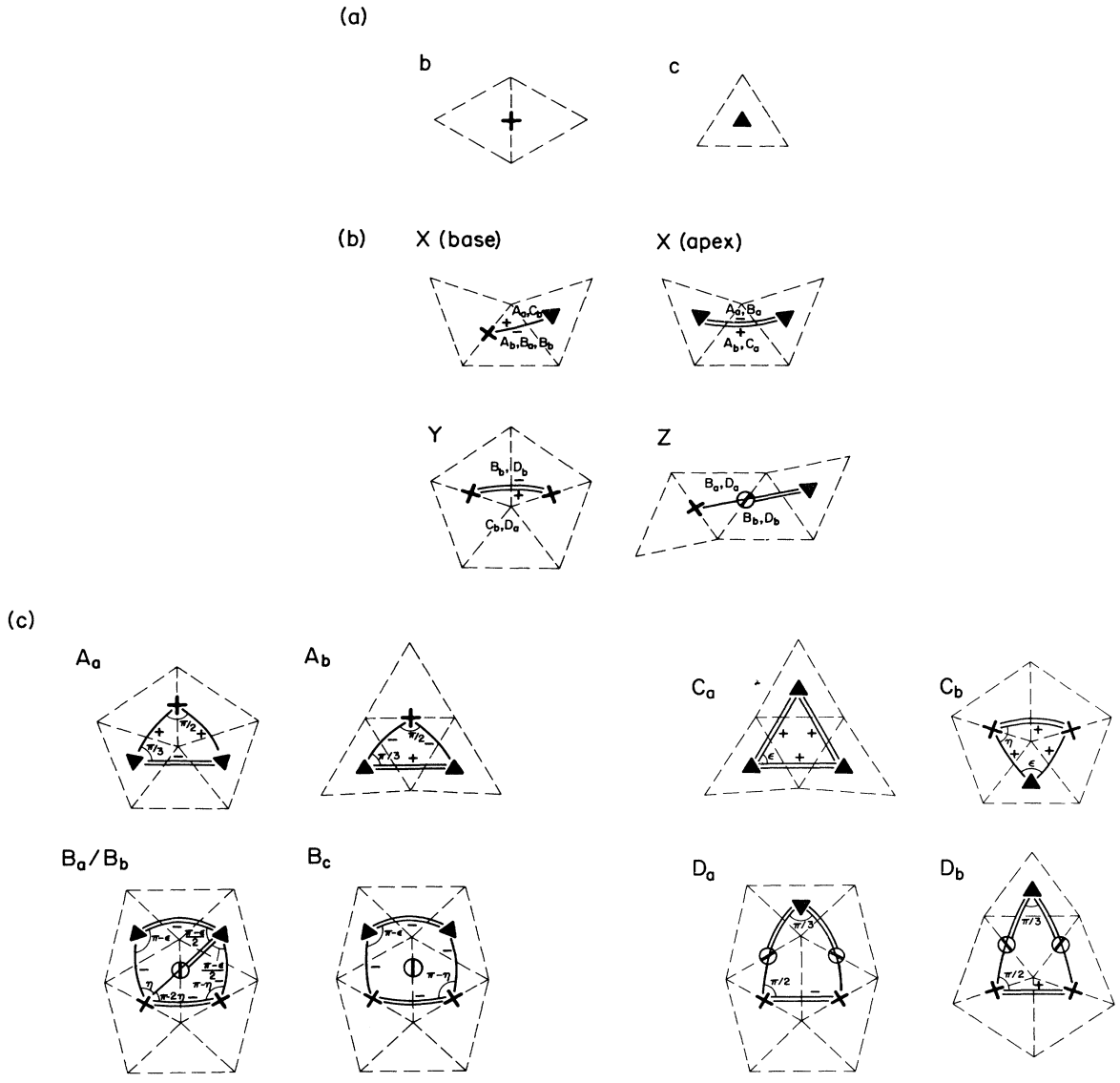

FIG. 5. (a) Bonds, (b) faces, and (c) cell corners around a vertex, become 2D spherical vertices, edges, and tiles when projected onto a sphere with icosahedral "coordinates" (dashed lines). A + on a given side of a 2D spherical edge means that the 3D cell on that side shows a face with a + marking. The circle with the heavy bar through it is the projection of the second-neighbor node diagonally across a Z face; the bar is the projection of the stub decoration through the Z face. Labels in (c) correspond to corner labels in Fig. 1. The 2D packing rules are indicated in (b) by the "A_a", etc., on the sides of the 2D spherical edges.

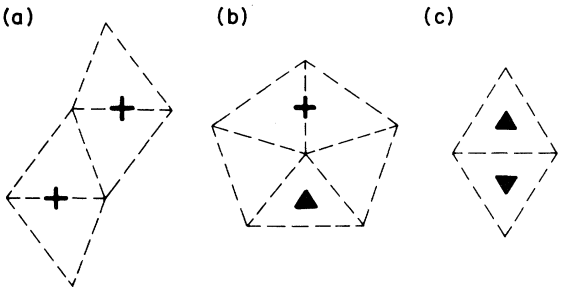

FIG. 6. Three arrangements forbidden in node local environments.

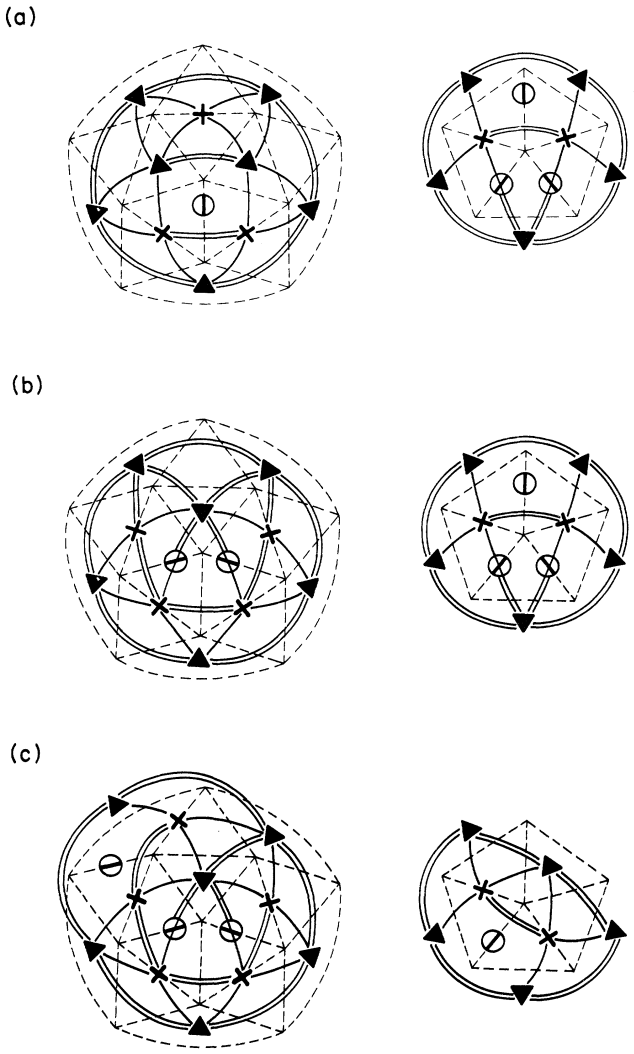

FIG. 7. Three of the 32 allowed node environments, shown using the conventions of Fig. 5. The reference icosahedron (dashed lines) is projected using an approximation of an equal-area projection with a "south pole" cap shown separately. (a) node $(57)_{3322}$, (b) node $(66)'_{4222}$, (c) node $(76)_{433}$. From each of (a) and (b), we can generate two other nodes by rotating the pentagonal "cap" on right.

the "south polar cap" in Fig. 7(a), and in each case $(\beta,\gamma)=(5,7)$ and $P=3$. Therefore, we append, as subscripts, the p counts for *every* fivefold direction (with $p>1$), in descending order. In a few cases this still leaves a pair of environments which would have the same label; in such a case one of them is given a superscript prime. These primed and unprimed pairs differ only by the rearrangement of one c linkage, except for the case of $(66)_{432}$ and $(66)'_{432}$.

Since, by icosahedral symmetry, most of the environments can have 120 distinct orientations, it is also useful to have a standard convention for orienting the picture. At the center of the front side, we place the icosahedron vertex with the largest number P of b linkages in a ring around it, and so that the mirror plane of that ring is vertical; this resolves most ambiguities of orientation.

C. Enumeration of allowed node types

We start by developing forcing rules which make it easy to recognize disallowed node types, and which lead to constraints on the 2D spherical tiling analogous to those of Sec. III A for the canonical-cell tiling.

1. Forcing rules at nodes

First we derive some "forcing rules" which must be obeyed by all local environments. The first refers to the sets of distances between neighboring nodes (analogous to the separations found in Ref. 46, Sec. IV A and Table IV, in the case of a quasiperiodic network).

Rule F0: Besides links b and c, the nearest allowed node separations are $\frac{1}{2}\sqrt{7}b\approx 1.323b$ and $\sqrt{2}b\approx 1.414b$.

Remark: The former is the diagonal of a Z face; the latter is the diagonal of two b linkages at right angles, formed whenever two A cells adjoin.

Proof: Obviously the only separations appearing within a single cell are $b,c\,(=\frac{1}{2}\sqrt{3}b)$ and $\frac{1}{2}\sqrt{7}b$; but surely any other separations less than $\sqrt{2}b$ must be relating nodes in neighboring cells. Thus, for each face, we need only consider the different ways of packing a cell on each side, and calculate the separations between the nodes (that are not in the faces) of the two cells. There are 11 combinations: $(A_+,C_+)X(A_-,B_-)$; $(C_+,D_+)Y(B_-,D_-)$; and $B(Z)B$, $B(Z)D$, or $D(Z)D$. The distances are all larger than those mentioned in rule $F0$.

TABLE IV. Solid angles of cell corners.

Corner	Solid angle	Number of bonds b	Number of bonds c
A_a	$\pi/6$	1/4	1/3
A_b	$\pi/6$	1/4	1/3
B_a	$\pi/2-3\epsilon/2+\eta$	$\eta/2\pi$	$3/4-3\epsilon/4\pi$
B_b	$3\pi/2-\epsilon/2-3\eta$	$1-3\eta/2\pi$	$1/4-\epsilon/4\pi$
B_c	$2(\pi-\epsilon-\eta)$	$1-\eta/\pi$	$1-\epsilon/\pi$
C_a	$3\epsilon-\pi$	0	$3\epsilon/2\pi$
C_b	$\epsilon+2\eta-\pi$	η/π	$\epsilon/2\pi$
D_a	$\pi/3$	1/2	1/6
D_b	$\pi/3$	1/2	1/6

The other rules apply to local environments. Here "triangle" means one of the 20 triangles of the icosahedron "coordinate system."

Rule F1: Unfilled triangles never adjoin.

Proof: Note "filled" was defined in Sec. III B 1. As noted there, emply triangles occur only in C_a and D_b corners, and an inspection of Fig. 5(c) shows that they are completely surrounded by filled triangles.

Rule F2: If a triangle is surrounded by triangles filled by b linkages, then it must be filled with a c link.

Proof: Otherwise, the triangle would stay empty. But C_a and D_b in Fig. 5(c) contain the only empty triangles, and, in either case, at least one neighboring triangle is filled by a c link.

Rules F3(a,b,c): Two linkages at a node cannot be related in the ways shown in Figs. 6(a)–6(c), respectively.

Proof: The impossibility follows from calculating the distances between the nodes at the ends of the two linkages. These are, respectively,

$$[(5/\sqrt{5})/2]^{1/2}b \approx 1.19b \ ,$$

$$[(9-2\sqrt{5})/4]^{1/2}b \approx 1.06b \ ,$$

and

$$\tau^{-1}b \approx 0.62b \ .$$

But, by rule $F0$, these cannot be separations between nodes in a canonical-cell tiling.

Rule F4: One cannot have five b linkages in a ring around a node.

Proof: This makes a spherical pentagon with five edges of the type labeled Y in Fig. 5(b), with + markings on the outside. Then, inside each edge must be either a B_b or D_a. But no two B_b can adjoin, and, at most, one can be a D_b since that includes the central five-fold corner; clearly there is no way to fill the pentagon.

As a byproduct of the classification of environments summarized in Sec. III C 3, we find that the forcing rules are not only necessary, but sufficient.

Theorem: Every arrangement of radial linkages that satisfies rules $F1-F3$ is a valid canonical-cell node.

Proof: By the complete enumeration of cases (see Appendix D).

2. *Sum rules for solid angles at a node*

Without considering the angular arrangement of objects around a node, we can count them two ways.

(i) We can count the numbers of each cell corner in the integer "eight-vector"

$$N(A_a, A_b, B_a, B_b, C_a, C_c, D_a, D_b) \ . \tag{3.12}$$

(Every B_c corner is considered to be broken down into B_a+B_b.)

(ii) We can count the numbers of b and c linkage ends, and the fraction k of the total area (i.e., solid angle) $\Omega(BC)$ occupied by B and C corners:

$$(\beta,\gamma,k) \equiv (N(b), N(c), \Omega(BC)/2\pi) \ . \tag{3.13}$$

We will see shortly that k is an integer and $k/2 = \frac{1}{2}$ in most local environments; note the close analogy between $1-k/2$ and the AD volume fraction μ of Eq. (3.5).

Obviously, given (3.12), we can find (3.13), given by a matrix equation with coefficients from Table IV:

$$\begin{bmatrix} \beta \\ \gamma \\ k \\ 1 \end{bmatrix} \equiv \begin{bmatrix} \frac{1}{4} & \frac{1}{4} & \frac{\eta}{\pi} & 1-\frac{3\eta}{\pi} & 0 & \frac{2\eta}{\pi} & \frac{1}{2} & \frac{1}{2} \\ \frac{1}{3} & \frac{1}{3} & \frac{3}{4}-\frac{3\epsilon}{\pi} & -\frac{\epsilon}{4\pi} & \frac{3\epsilon}{2\pi} & \frac{\epsilon}{2\pi} & \frac{1}{6} & \frac{1}{6} \\ 0 & 0 & \frac{1}{8}+\frac{\eta}{4\pi}-\frac{3\epsilon}{8\pi} & \frac{3}{8}-\frac{3\eta}{4\pi}-\frac{\epsilon}{8\pi} & -\frac{1}{4}+\frac{3\epsilon}{4\pi} & -\frac{1}{4}+\frac{\eta}{2\pi}+\frac{\epsilon}{4\pi} & 0 & 0 \\ \frac{1}{24} & \frac{1}{24} & \frac{1}{8}+\frac{\eta}{4\pi}-\frac{3\epsilon}{8\pi} & \frac{3}{8}-\frac{3\eta}{4\pi}-\frac{\epsilon}{8\pi} & -\frac{1}{4}+\frac{3\epsilon}{4\pi} & -\frac{1}{4}+\frac{\eta}{2\pi}+\frac{\epsilon}{4\pi} & \frac{1}{12} & \frac{1}{12} \end{bmatrix}$$

$$\times \begin{bmatrix} N(A_a) \\ N(A_b) \\ N(B_a) \\ N(B_b) \\ N(C_a) \\ N(C_b) \\ B(D_a) \\ N(D_d) \end{bmatrix} \ . \tag{3.14}$$

The last row is the fraction of total solid angle occupied by corners, which must be unity.

As in the quasiperiodic "3D Penrose tiling" [Ref. 46, Eq. (B2)], but less easily, it will turn out we can invert this and derive (3.12) given (3.13). That is, given the values (β,γ,k) of an environment, there is only one possible set of numbers

$(N(A_a),N(A_b),\ldots)$ independent of the several ways the linkages might be arranged.

We first derive more linear equations in the spirit of the 3D sum rules of Sec. III A. Note [Fig. 5(b)] that, there, each of the four kinds of 2D edges has a + and a − side. For each face type α, the sum

$$W_\alpha = w_\alpha(A_a)N(A_a)+w_\alpha(A_b)N(A_b)+\cdots+w_\alpha(D_b)N(D_b)=0\ ,$$

where the weight $w_\alpha(T)$ is the signed number of 2D edges from face type α appearing around the 2D spherical tile "T." The coefficients $w_\alpha(\ )$ can be written in matrix form:

$$\begin{bmatrix} W(X(\text{base})) \\ W(X(\text{apex})) \\ W(Y) \\ W(Z) \end{bmatrix} = \begin{bmatrix} 2 & -2 & -1 & -1 & 0 & 2 & 0 & 0 \\ -1 & 1 & -1 & 0 & 3 & 0 & 0 & 0 \\ 0 & 0 & 0 & -1 & 0 & 1 & -1 & 1 \\ 0 & 0 & 1 & -1 & 0 & 0 & 2 & -2 \end{bmatrix} N(A_a,A_b,B_a,B_b,C_a,C_b,D_a,D_b) = \begin{bmatrix} 0 \\ 0 \\ 0 \\ 0 \end{bmatrix} . \tag{3.15}$$

One can now derive two equations by elimination in (3.15). The same equations also follow by noting that the sums in (3.14) are integer although the ϵ and η terms in (3.14) are irrational; hence, their coefficients must be identically zero:

$$\begin{bmatrix} -3 & -1 & 6 & 2 \\ 1 & -3 & 0 & 2 \end{bmatrix} N(B_a,B_b,C_a,C_b) = \begin{bmatrix} 0 \\ 0 \end{bmatrix} . \tag{3.16}$$

The solutions in integers of (3.16) are

$$N(B_a,B_b,C_a,C_b)=(4,2,2,1)k+(-1,1,-1,2)l\ , \tag{3.17}$$

where k,l are integers. Substitution into (3.14) confirms that k in (3.17) is the same as the k in (3.12). Since k is an integer, either (i) $k=0$, there are *no* B/C corners, (ii) $k=1$, A/D and B/C corners each occupy exactly *half* the solid angle, or (iii) $k=2$, B/C corners occupy *all* of the solid angle.

Now, an A cell cannot adjoin on a D cell. Thus, if [case (i)] there are no B/C corners, then the corners must either be all A_x or all D_x; this forces the nodes found in the A and D crystalline structures, respectively. Similarly, if [case (iii)] there are only B/C corners, this forces the node of the BC crystalline structure $[(k,l)=(2,2)]$.

Inserting (3.17) back into (3.12)–(3.14), we now obtain

$$\beta=6-k+l\ , \tag{3.18a}$$

$$\gamma=8-\tfrac{1}{2}\{k+l+[N(D_a)+N(D_b)]\}\ . \tag{3.18b}$$

Hence,

$$l=(\beta-5)k\equiv\beta-6+k\ . \tag{3.19}$$

[Note that all three cases with $k\neq1$ have $\beta=6$, so that $(\beta-6)(k-1)\equiv0$ can be used as an identity.] From this we get the values of $N(B_a,B_b,C_a,C_b)$ given below.

So far, two linearly independent equations from the set (3.15) have not been used. Substitution into these gives

$$\tfrac{1}{2}[N(A_a)-N(A_b)]=N(D_b)-N(D_a)=6-\beta\ . \tag{3.20}$$

Furthermore, substitution into the solid-angle equation (3.14) now tells us

$$[N(A_a)+N(A_b)]+2[N(D_a)+N(D_b)]=24(1-k/2)\ , \tag{3.21}$$

which, coupled with (3.18b), yields $N(A_a)+N(B_b)$ and the full solution

$$\begin{aligned} N(A_a)&=2(\gamma-2-2k)\ , \\ N(A_b)&=2(\beta+\gamma-8-2k)\ , \\ N(B_a)&=3k-\beta+6\equiv(9-\beta)k\ , \\ N(B_b)&=3k+\beta-6\equiv(\beta-3)k\ , \\ N(C_a)&=k-\beta+6\equiv(7-\beta)k\ , \\ N(C_b)&=3k+2\beta-12\equiv(2\beta-9)k\ , \\ N(D_a)&=8-\gamma-k\ , \\ N(D_b)&=14-\beta-\gamma-k\ . \end{aligned} \tag{3.22}$$

[We could have anticipated the appearance of three parameters (β,γ,k) in the solution, since we had five independent equations (3.14) and (3.15) in eight unknowns.] Of course, $N(\cdots)\geq0$, so Eqs. (3.22) imply the inequalities

$$5\leq\beta\leq7,\quad 4\leq\gamma\leq7,\quad 10\leq\beta+\gamma\leq13\ . \tag{3.23}$$

In all, 13 possible combinations (β,γ) are realized in node environments. Their contents, as calculated from (3.22), are given in Table V. [The cases with $k=1$ and $(\beta,\gamma)=(5,5)$ or (7,4), although allowed by (3.23), do not occur in any environment.]

3. *Exhaustive enumeration of allowed node types*

As just noted above, the only nontrivial case is $k=1$ where half the solid angle is BC corners and the other half is AD corners. The inequalities (3.23) restrict the possible values of (β,γ,k), thus reducing the work of ex-

TABLE V. Cell corners in node environments.

(N_bN_c)	k	A_a	A_b	B_a	B_b	C_a	C_b	D_a	D_b	Number of environments
(68)	0	12	12	0	0	0	0	0	0	1
(64)	1	0	0	3	3	1	3	3	3	1
(62)	0	0	0	0	0	0	0	6	6	1
(56)	1	4	2	4	2	2	1	1	2	3
(57)	1	6	4	4	2	2	1	0	1	3
(64)	1	0	0	3	3	1	3	3	3	2
(65)	1	2	2	3	3	1	3	2	2	3
(66)	2	0	0	6	6	2	6	0	0	1
(66)	1	4	4	3	3	1	3	1	1	10
(67)	1	6	6	3	3	1	3	0	0	3
(75)	1	2	4	2	4	0	5	2	1	4
(76)	1	4	6	2	4	0	5	1	0	1

TABLE VI. Allowed node environments.

Name	Symmetry	Type	Figure
$(68)_0$	$2/m\bar{3}$	pure A (1/1 cubic)	13(a) and 14
$(64)_{222222}$	$3m$	Y plane	13(b)
$(62)_{222222}$	$\bar{3}m$	pure D	13(a) and 14
$(56)_{222}$	m	b wedge	13(c)
$(56)_{322}$	1		
$(56)_{422}$	m		
$(57)_{322}$	1		7(a), rotated
$(57)_{332}$	1		7(a), rotated
$(57)_{3322}$	m		7(a)
$(64)_{3322}$	m	Z plane	13(b) and 14
$(64)'_{3322}$	m	b wedge	13(c)
$(65)_{432}$	1		
$(65)_{3322}$	1	c wedge	14
$(65)'_{3322}$	1		
$(66)_{222222}$	$\bar{3}m$	BC	13(a) and 14
$(66)_{3332}$	1		
$(66)_{333}$	1		
$(66)_{422}$	1	c wedge	14
$(66)_{4222}$	m	c wedge	14
$(66)'_{4222}$	m		7(b)
$(66)_{432}$	1		7(b), rotated
$(66)'_{432}$	1		
$(66)_{4322}$	1		
$(66)'_{4322}$	1		7(b), rotated
$(67)_{322}$	m	X plane	13(b) and 14
$(67)_{332}$		c wedge	14
$(67)_{333}$	3	2/1 cubic	
$(75)_{3333}$	m	b wedge	13(b)
$(75)_{4332}$			
$(75)'_{4332}$			
$(75)_{4422}$			
$(76)_{433}$			7(c)

haustive enumeration.

To finish classifying the environments, we must now consider the ways in which link ends and cell corners are arranged around the solid angle, case by case. By systematically constructing (by hand) a "tree" of all possible cases, I found a total of 32 distinct environments, as tabulated in Table VI. The tree can be based on either (i) cell corners or (ii) link ends, as detailed in Appendix D. Figure 7 illustrates some common environments. By rotating the pentagonal "cap" on the right, Fig. 7(a) also produces $(57)_{322}$ and $(57)_{332}$; similarly, Fig. 7(b) also produces $(66)'_{4322}$ and $(66)_{432}$.

IV. PERIODIC, LAYERED, AND TWINNED STRUCTURES

The canonical cells can be packed to form periodic as well as aperiodic structures. This is relevant for several reasons.

(i) Decorating a periodic packing provides a trial atomic model for several large unit-cell approximants which have recently been discovered by electron diffraction (Sec. IV A). However, contrary to an earlier suggestion,[66] most of the large-cell structures found in Al–transition-metal phase diagrams near the quasicrystal-forming concentration are *not* true approximants.

(ii) Since (Sec. V A) we do not yet know how to construct quasiperiodic canonical-cell structures, we must use periodic structures to approximate them and to obtain some suggestive information about their statistical geometry, e.g., counting the distributions of the different kinds of node local environments, or in modeling the real-space atomic structure.[67] Furthermore, periodic boundary conditions are desirable for technical reasons in calculations of physical properties.[4,68] Some examples are the following: electronic structure calculations,[68] dependence of diffraction on atomic decoration,[34] or modeling of surface structure.[69,70]

Some special grain boundaries are known which allow joining domains of different periodic canonical-cell packings without any violation of the canonical-cell rules. We do not believe that most icosahedral "quasicrystals" are really twinned aggregates of crystals in this fashion. However, the large approximants in nature[35,37] do occur microtwinned and it is interesting to explore how defective the structure must be along a grain boundary (Sec. IV E).

A. Approximants in nature

The cubic "approximants" α(Al-Mn-Si) and R(Al-Cu-Li) have been starting point for models of the different atomic arrangements of the i(Al-Mn) and i(Al-Zn-Mg) classes, respectively. But in terms of the description used in this paper, they appear rather trivial, consisting of a bcc packing of icosahedral clusters, and containing only A canonical cells. Recently several *larger* approximants have been discovered, with cells larger than the bcc packing and closely related to the icosahedral phase (as observed from the similarity of electron-diffraction patterns).

Note that, by our linkage rules, *all* the clusters decorating icosahedral node centers must be oriented the same way, so the point group of a periodic packing must be a subset of the icosahedral point group. This greatly restricts the possibilities for the space group: there are *no* true tetragonal or hexagonal structures.[71] (In orthorhombic, rhombohedral, and cubic structures, the point groups are at most $2/mmm$, $\bar{3}2/m$, and $2/m\bar{3}$, respectively.) In the i(Al-Mn) system, at compositions close to the quasicrystals, a few large unit-cell compounds (still unsolved by x-ray diffraction) were speculated to be approximants.[66,72] but most of them are supposed to have point groups incompatible with a single orientation of the icosahedral clusters.[66]

Recently, genuine large-cell approximants have been discovered. In the i(Al-Mn) structure class, the equilibrium quasicrystal i(Al-Cu-Fe) was found to transform at lower temperatures to a rhombohedral crystal approximant.[37] This might be described as a packing of τ^3 inflated prolate Ammann rhombohedra decorated with clusters, with the cell then doubled due to the even-odd alternation mentioned in Sec. V B 2, below. Furthermore, five large-cell approximants (including the 3/2 approximant of Sec. IV C) were recently discovered in the Ga-Mg-Zn system.[35]

B. Simple periodic packings

For each of the three independent types of unit cell, there is a unique way to build a periodic packing with only that kind of cell. [Because of the constraint $n(B) \equiv n(C)$ found in Sec. III, we cannot independently pack B or C cells, but only an equal mix of the two.] The uniqueness is trivial to show: for each face of an A, B, or D cell, there is only one way to pack another A, C, or D cell, respectively. I will call these structures the "A," "BC," and "D" packings.

1. A packing

Using only A cells gives a bcc structure (space group $Im\bar{3}$); the nodes form a bcc Bravais lattice. This has the highest possible packing fraction of any possible packing of canonical cells (Table III). The *primitive* unit cell is the oblate rhombohedron of six A cells shown in Fig. 8(a). Each face is a rhombus made from two X faces.

If we take the bcc "A" structure and decompose it into Ammann rhombohedra as prescribed in Sec. II, it forms exactly a 1/1 cubic tiling with lattice constant b. The atomic structures of α-(Al-Mn-Si) (Refs. 4 and 38) as well as $(Al,Zn,Cu)_{49}(Mg,Li)_{32}$ (Ref. 6) were described as decorations of this rhombohedral tiling; however, the cluster description is simpler and more fruitful.

2. BC packing

Assume we have only B and C cells. Then each rectangular Z face of a B cell must adjoin on another B, so they form the trigonal antiprism (a flattened octahedron) B_2. Also, only a C cell can be placed on the triangular Y faces of the B_2. Thus, the absence of D's forces B's and C's to occur in "B_2C_2" units in a prolate rhombohedron shape [Fig. 8(b)]. Each face is a rhombus identical to the faces of the A_6 rhombohedron. These are *not* the same shape as the Ammann rhombohedra (see Sec. IV C, below). Thus, the only possible structure is the rhom-

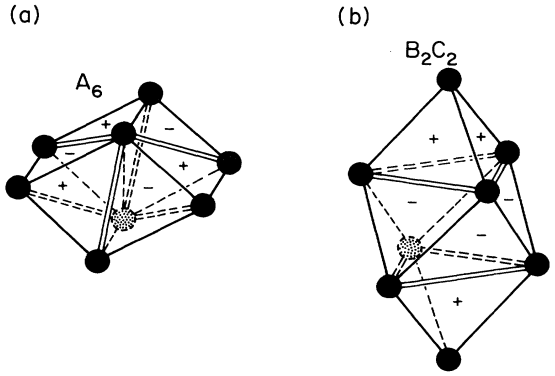

FIG. 8. Rhombohedral primitive cells of periodic structures. (a) Oblate rhombohedron of "A" structure. (b) Prolate rhombohedron of "BC" structure.

bohedral BC packing mentioned in Sec. II B, for which the B_2C_2 cluster is the unit cell.

3. *D packing*

In this structure the cells occur alternately in just two orientations; the nodes form a hexagonal Bravais lattice (stacked triangular layers).

C. Large cubic cells

1. *Cubic packings of Ammann rhombohedra*

It is well known that the projection method for generating the rhombohedral 3D Penrose tiling can be adapted to produce periodic approximant tilings by using a projection strip which is oriented in a commensurate direction, as described in Ref. 4 and also Ref. 27. There is a sequence of such structures which are called "F_n/F_{n-1} cubic" (where F_n denotes the nth Fibonacci number: $F_1=1$, $F_2=2,\ldots$). An F_n/F_{n-1} cubic approximant has cubic lattice constant $a_c=\tau^{n-1}b$; it contains F_{3n+1} prolate and F_{3n} oblate rhombohedra. It is easy to check that the volume of the unit cell can be expressed as[73]

$$\tau^{3n}b^3=(F_{3n+1}\tau^{-1}+F_{3n}\tau^{-2})b^3 \ . \tag{4.1}$$

Of course, noncubic approximants are possible too.

Thus, given an atomic-structure model based on decorating Ammann rhombohedra with atoms, one can trivially generate approximants of arbitrarily large size. Here, however, we will instead construct some particular periodic packings of canonical cells (it is not clear exactly what these are "approximating," nor do we have a general rule to construct arbitrarily large approximants). These will be given the same label F_n/F_{n-1} as the packing of Ammann rhombohedra (with a quasilattice constant of $a_r\sim 5$ Å) *having the same unit cell.* Table VII gives the data on the cell contents for some periodic structures.

Since (Sec. V A) a perfect quasiperiodic canonical-cell tiling has not yet been formulated, we commit an abuse of language in calling the canonical-cell packings discussed below "approximants." The abuse is small, however, for canonical-cell packings with moderate-sized unit cells which happen to be approximants (in the strict sense) of the quasiperiodic twelve-fold packing (Appendix B). This is the case of the 3/2 cubic approximant[74] (Sec. IV C 3), and is probably so for every entry in Table VII. (For larger approximants, though, it cannot be true, since Table III shows the twelve-fold packing has a much lower packing fraction than a canonical-cell packing.)

2. *Small cubic approximants*

We start by describing a way of packing eight rhombohedra into a unit cell, which works for arbitrary angles of the rhombohedra; this is needed in order to describe two nontrivial approximants based on two different sets of rhombohedron shapes.

In order to pack the rhombohedra together, it is necessary (and sufficient) that their faces are identical rhombuses. For any given acute rhombus angle θ, there is one way to make a prolate rhombohedron and one way to make an oblate rhombohedron, using that rhombus for the faces. If c_+ and c_- are the threefold axes of prolate and oblate rhombohedra, respectively, then

$$c_+/c_-=(1+2\cos\theta)^{1/2}/(1-2\cos\theta)^{1/2} \ . \tag{4.2}$$

There is always a cubic packing of four prolates and four oblates per unit cell in the nonsymmorphic simple-cubic space group $Pa\bar{3}$. In this space group, the $\langle 111\rangle$ threefold symmetry axes in different directions do *not* intersect (the group is nonsymmorphic). In each unit cell, each threefold axis of $Pa\bar{3}$ is the central threefold axis of one oblate rhombohedron and one prolate rhombohedron. These span the cubic unit cell, tip to tip, so that

$$c_++c_-=\sqrt{3}a_{\rm cub} \ , \tag{4.3}$$

where $a_{\rm cub}$ is the lattice constant. The maximum symmetry points are the centers of the prolates and oblates. These form complementary fcc structures as in a CsCl structure. All prolates are surrounded by oblates and vice versa. There is a handedness to the structure as we look down a threefold axis since there are two ways (related by mirror symmetry) to pack oblate rhombohedra around the faces of a prolate rhombohedron. The eight rhombohedron vertices are at crystallographically equivalent sites in class "8c" at $[x,x,x]$, where

$$x=c_-/2(c_++c_-) \ . \tag{4.4}$$

In particular, this packing can be made from the Ammann rhombohedra of the three-dimensional Penrose tiling.[23,24,26,27] They have edges along fivefold directions and

$$\theta=\cos^{-1}(1/\sqrt{5})=63.43^\circ \ .$$

Thus, Eq. (4.2) gives $c_+/c_-=\tau^3$ and (4.4) gives $x=\tau^{-2}/4$. For Ammann rhombohedra of edge a_R, this produces the 1/0 tiling described by Kuriyama and Long;[75] its cell is too small for a canonical-cell packing. For inflated Ammann rhombohedra of edge τ^3a_R, it pro-

duces the 3/2 tiling, the largest one we have studied (see below).

Such a packing can also be made from the A_6 and B_2C_2 rhombohedral unis described in Sec. IV B 2 above, and shown in Fig. 8. Their edges are along icosahedral threefold symmetry directions and

$$\theta=\cos^{-1}(1/3)=70.53^\circ .$$

Hence, by (4.2), $c_+/c_-=\sqrt{5}$ and by (4.4) the vertex coordinates are at $x=\tau^{-1}/4$. This is the "*ABC*" (=2/1) canonical-cell packing.

3. *The 3/2 cubic packing*

Elser has discovered a packing of *A*, *B*, *C*, and *D* canonical cells, with lattice constant $\tau^2 b$. This has 32 nodes per unit cell; when decorated with atoms, it produces a structure model with lattice constant over 30 Å and some 2000 atoms per unit cell.[74]

We can best understand the 3/2 packing by starting with the 1/0 packing of Ammann rhombohedra, then inflating it by a factor τ^3, and viewing the canonical cells as a decoration of these large rhombohedra;[76] this decoration (shown in Figs. 9 and 10) is very symmetrical.

TABLE VII. Periodic structures.

Name	Space group	Lattice constant(s)	Cell contents *A*	*BC*	*D*	$\mu-\frac{1}{2}$	ζ	Node position	Node type
1/1 cubic	$Im\bar{3}$	$a_{cub}=b$	12	0	0	$\frac{1}{2}$	0	2(a) in (0,0,0)	(68)
BC[a]	$R\bar{3}m$	$a_{rh}=c$, $\alpha_{rh}=70.53^\circ$	0	2	0	$-\frac{1}{2}$		1(a) in (0,0,0)	$(66)_{222222}$
D	$P\bar{3}m1$	$a_{hex}=b$, $c_{hex}=c$	0	0	2	$\frac{1}{2}$	1	1(a) in (0,0,0)	$(62)_{222222}$
2/1 cubic	$Pa\bar{3}$	$a_{cub}=\tau b$	24	8	0	$-\frac{1}{2}\tau^{-6}$	0	8(c) in (x,x,x), $x=\tau^{-1}/4$	$(67)_{333}$
3/2 cubic	$Pa\bar{3}$	$a_{cub}=\tau^2 b$	72	32	8	$\frac{1}{2}\tau^{-12}$	0.333	8(c) in (x,x,x), $x=\tau^{-2}/4$	$(67)_{333}$
								24(d) in $(\sqrt{5},-\sqrt{5},-1)\tau^{-2}/4$	$(66)'_{4322}$
$(2/1)^2\times 1/1$ orthorhombic	$Pnma$	$a_0=c_0=\tau b$, $b_0=b$	0	4	4	$\frac{1}{2}\tau^{-4}$	1	4(c) in $(\sqrt{5},0,1)\tau^{-1}/4$	$(64)'_{3322}$
$(2/1)^2\times 3/2$ monoclinic	$P2_1/c$	$a_{mono}=\tau^2 b$, $b_{mono}=c_{mono}=\tau b$, $\beta_{mono}=90^\circ$	24	12	4	$\frac{1}{2}\tau^{-8}$	0.429	4(e) in $(-\tau^{-2},\tau^{-1},\tau^{-1})/4$	$(65)'_{3322}$
								4(e) in $(3\tau^{-2},\tau^{-1},\tau^{-1})/4$	$(66)_{4322}$
								4(e) in $(\frac{1}{2},0,\frac{1}{2})+(\tau^{-2},\tau^{-1},-\tau^{-1})\tau^{-1}/4$	$(67)_{333}$
$(2/1)^2\times 3/2$ orthorhombic[b]	$Cmc2_1$	$a_0=\tau^2 b$, $b_0=c_0=\tau b$	24	12	4	$\frac{1}{2}\tau^{-8}$	0.429	4(a) in $(0,\tau^{-2},-\tau^{-1})/4$	$(66)'_{4222}$
								8(b) in $(\tau^{-2},\tau,\tau^{-1})/4$	$(66)_{4322}$
$(2/1)^2\times\tau$ "orthorhombic"	...	$a_0=b_0=\tau b$, $c_0=\infty$				0	0.317		
3/2-OR[c]	$R3m$	$a_{rh}=\tau^3 a_R$, $\alpha_{rh}=116.57^\circ$	6	3	1	$\frac{1}{2}\tau^{-8}$	0.429	3(b) in $(\tau^{-2},0,0)$	$(66)_{4222}$
Figure 13(c)	$P\bar{3}$	$a_{hex}=\sqrt{2}\tau b$, $c_{hex}=c$	18	6	2	$\frac{1}{2}\tau^{-4}$	0.333	1(a) in (0,0,0)	$(68)_0$
								6(g) in $(\frac{1}{2},0,0)+(-\tau^{-1},\tau^{-1},1)/3$	$(66)_{422}$

[a]In hexagonal coordinates, $a_{hex}=b$ and $c_{hex}=\sqrt{5}c$.
[b]Ohashi, Ref. 35.
[c]In hexagonal coordinates, $a_{hex}=\tau^2 b$ and $c_{hex}=c$.

Every vertex is a node; also, two nodes are associated with every face, one on the face and the other above or below it [Fig. 9(c)]. In the case of the large OR, the node *below* a face on one side is also *on* one of the faces on the opposite side of the OR. Note the similarities of Fig. 10 here to Fig. 16 of Ref. 46, which showed the "twelvefold" sites as a decoration of the τ^3-inflated rhombohedra in the 3DPT.

Along each threefold axis of the 3/2 structure, we have alternating large oblate and prolate rhombohedra. As can be seen from Fig. 9, this implies the following sequence of canonical cells along the threefold axis: A_6, C, D, B_2, D, C, A_6, C etc. The high-symmetry points (0,0,0) and $(\frac{1}{2},\frac{1}{2},\frac{1}{2})$ are at the centers of the A_6 cluster and the B_2. There are several other crystallographically inequivalent cells filling the spaces between the threefold axes.

D. Layered structures

Here we consider canonical-cell structures which have a b or c bond displacement (stacking vector) as a period in one direction, but which have long periods (or are aperiodic) in the other two. Thus, they consist of layers stacked along an icosahedral twofold or threefold axis. To represent the structure, we project columns of cells along the stacking axis onto two-dimensional polygons; these form a tiling. Each polygon represents a cluster of one to six cells which, together, make up the parallelpiped which is obtained by translating a tilted face vertically by the stacking vector. Every node has b (or, respectively, c) bonds extending above and below in the stacking direction; consequently, all other allowed bonds are inclined well away from these directions.

Stackings in this fashion would provide models for the supposed $(Ti_{1-x}Ni_x)_2V$ phase,[77] stacked in a twofold direction, and the T'(Al-Mn) phase, stacked in a threefold direction,[72] both of which were claimed to be incommensurate normal to the stacking direction.

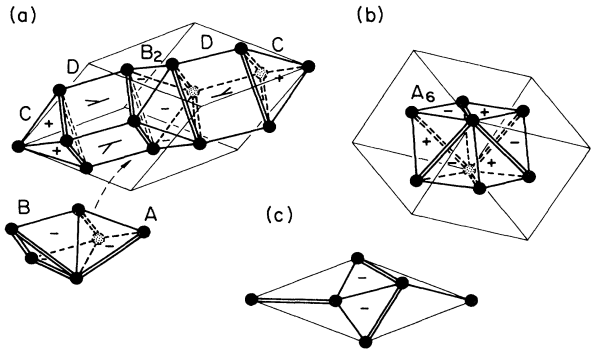

FIG. 9. Parts of the 3/2 cubic packing of canonical cells, shown relative to the outlines of the "large" (τ^3-inflated) Ammann rhombohedra: (a) large oblate rhombohedron, (b) large prolate rhombohedron. These alternate along the threefold axes of the cubic cell. All other canonical cells border on, and are forced by, the ones shown. Every large rhombohedron face is decorated as in (c): one node is in the face and the other is offset normal to it.

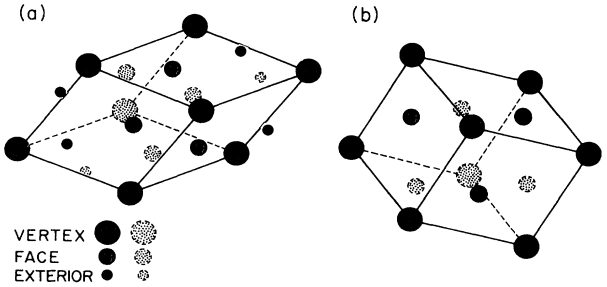

FIG. 10. The same nodes as in Fig. 9 are presented so as to emphasize that the decoration is similar to that of Ref. 46, Fig. 16, but more symmetrical.

1. *Twofold (b) axis*

The bonds within the layers normal to the twofold axis project to three kinds of tiling edges [Fig. 11(a)]. One kind, of length $(1/\sqrt{2})b$, is the projection of c bonds which (with the vertical b bonds) form X faces. Two kinds are of length $(\sqrt{3}/2)b$ but they are unrelated: one of these kinds is a projection of b bonds which (with the vertical b bonds) form Y faces, the other is a projection of horizontal c bonds which (with the vertical b bonds) form Z faces.

These form three kinds of tiles in the two-dimensional projection [Fig. 11(b)]. There is a square of edges $(1/\sqrt{2})b$, which is a projection of a cluster A_6; an isosceles triangle with acute angle $\pi-2\eta$, where η is the angle defined in Sec. II, which is the projection of a cluster BC, and a larger square with inequivalent kinds of edges of length $(\sqrt{3}/2)b$, which is the projection of a cluster D_2.

The three-dimensional packing rules of the cells induce two-dimensional packing rules of these tiles, which are implemented by the slashes shown along the edges in Fig. 13(b). There is a one-to-one correspondence between two-dimensional tilings satisfying the packing rules and b-layered structures. There is also a one-to-one correspondence with triangle-square tilings (compare the patterns in Figs. 13 and 16).] The simple periodic structures discussed above—the A, BC, and D packings—are all special cases of b-stacked structures; they are represented by tilings which are just repetitions of the respective patterns in Fig. 13(a).

An interesting periodic packing stacked along a b axis is the $(2/1)^2\times(1/2)$ orthorhombic approximant shown in Fig. 15(a). Note that although $a_0=b_0$, the structure is not tetragonal (the edges of the 2D square tiles, representing columns of D cells, are certainly not equivalent). In the same way, Ohashi's c-face-centered $(2/1)^2\times(3/2)$ approximant is only orthorhombic; it is the favored structural model for the observed approximant in Ga-Mg-Zn,[35] which shows the same systematic absences. By stacking a (2/1) cubic cell on top of the $(2/1)^2\times(1/2)$ orthorhombic cell, a different $(2/1)^2\times(3/2)$ approximant is produced; this structure has the same shape of unit cell, but is officially only monoclinic since the contents are packed less symmetrically. We can also stack thin (b) and fat (τb) layers in a *quasiperiodic* Fibonacci sequence on the $\tau b\times\tau b$ base to make a "$(2/1)\times\infty$" approximant (see Table VII).

2. *Stackings along threefold (c) axis*

The vertical faces of these structures project to just two kinds of 2D tile edge. There are edges of length $\sqrt{2/3}b$, projected from b and c bonds which (with the vertical b bonds) form X faces [Fig. 12(a)]; the other kind of edge is of length b, projected from a horizontal b bond. The decorations here are different from the b-stacked case, because the twofold axis is normal to a mirror plane but the threefold axis is not. The arrows indicate which way is down along the c bond.

There are again three kinds of tile [Fig. 11(b)]: (i) An equilateral triangle with edges $\sqrt{2/3}b$, projected from a cluster A_3 (the column of stacked A_3's has a threefold screw axis). (ii) An isosceles triangle with apex angle ϵ, projected from a BC combination. (iii) A larger, horizontal, equilateral triangle of edge b, projected from a D cell.

The simple A, BC, and D packings are special cases of c-stacked structures. The corresponding 2D tilings are repetitions of the patterns in the first row of Fig. 14.

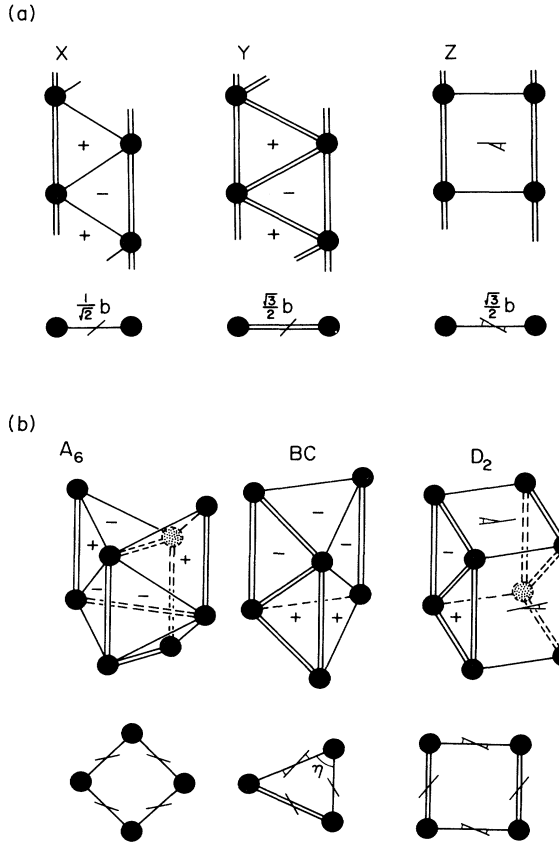

FIG. 11. Faces and cells of structures stacked along a twofold (b-bond) axis, projected onto a normal layer, and represented as edges and polygons of a two-dimensional tiling. Each solid circle in the two-dimensional tiling represents a column of nodes connected by b bonds. (a) Allowed stacks of faces become 2D edges, with lengths indicated and with slashes representing 2D packing rules (b). Allowed stacks of cells become 2D tiles. Notice how the fourfold symmetry of the A_6 and D_2 squares and the mirror symmetry of the BC isosceles triangle are broken.

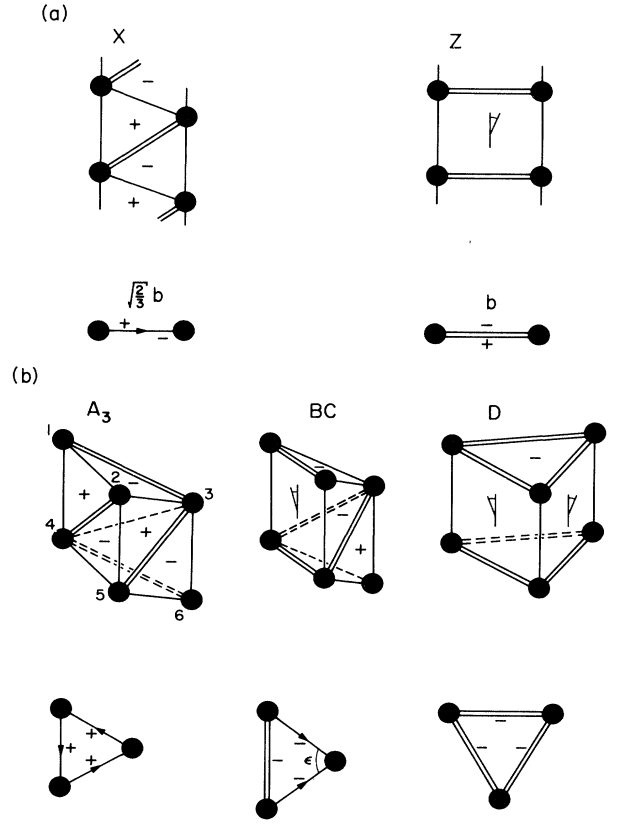

FIG. 12. Faces and cells of structures stacked along a threefold (c-bond) axis, as in Fig. 11. (a) Allowed stacks of faces; arrow on the 2D edges marks downward direction of (nonvertical) c bonds. (b) Allowed stacks of cells.

The next simplest c-stacked structure is the (3/2)-OR rhombohedral structure shown in Fig. 15(b). The unit cell has the same size and shape as the τ^3-inflated oblate Ammann rhombohedron in Fig. 9, but in this case the nodes are not on the high-symmetry corner points. (This packing gives a more attractive model for the observed Ga-Mg-Zn approximant than Ohashi's model,[35] which includes close distances between clusters along, e.g., fivefold axes, and thus violates canonical-cell rules.)

Another c-stacked structure is shown in Fig. 15(c). Note how the projection of its cluster centers is a simple triangular net with a $\sqrt{7}\times\sqrt{7}$ distortion. For this reason, Guyot and Audier suggested it[78] as a model for $\lambda(Al_4Mn)$.

E. Twinned structures and grain boundaries

1. *Quasicrystal versus twinning models*

Noncrystallographic diffraction patterns cannot all be explained by twinning moderately large ($\sim$30 Å) unit-cell crystals.[79] Twinning of structures with much larger cells would be consistent with experiment only if the unit cell were identical to a portion of a quasicrystal structure; in this case the structure is more economically described as an approximant to a quasicrystal. On the other hand,

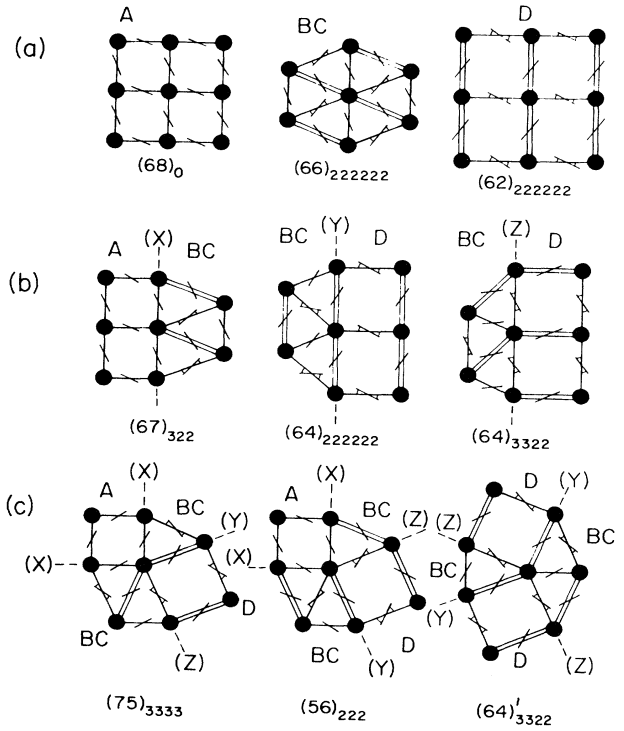

FIG. 13. Allowed nodes in *b*-stacked structures: (a) Nodes from pure periodic structures, (b) grain-boundary nodes, (c) wedge nodes. The name of the node type is given beneath. Arrangements in (b) and (c) can be extended to infinity using grain boundaries along the dashed lines.

since each kind of canonical cell can be packed in a periodic structure, one might be tempted to call the random tiling of cells a "microtwinned" structure. However, this can be distinguished, in principle, by its diffraction properties: in a *twinning* explanation, the whole diffraction pattern is an *incoherent* superposition of rotated, broadened copies of a single crystal's spots. The random-tiling diffraction pattern includes spots due wholly to *coherent* interference between different cells, i.e., longer-range correlations. In some experimental systems, twinned structures appear to grade continuously into random quasicrystal structures.[80,81]

2. *Grain boundaries and their intersections*

Now let us consider ways we might fill space with periodic structures which satisfy *perfectly* the canonical-cell rules, even at the grain boundaries. In view of the preceding paragraph, these must be domains of more than one kind of periodic structure.

Grain boundaries are only possible between A and BC, or between BC and D packings. For (Sec. III B), when we pack with purely A, purely BC, or purely D cells, the entire structure is determined. Also, the A and D structures have no kind of face in common.

A boundary plane can be made from X, Y, or Z faces (Fig. 11); such planes occur within the simple packings as follows: (i) X planes are (110) faces of the bcc A structure and they are (100) faces of the rhombohedral BC structure. (ii) Y planes are (111) faces of the rhombohedral BC structure and (001) faces of the trigonal D structure. (iii) The rectangular Z planes form (110) planes of the rhombohedral BC structure and (110) planes of the trigonal D structure. Thus, there are three types of grain boundaries: (i) $A(X)BC$, (ii) $BC(Y)D$, and (iii) $BC(Z)D$, where the intervening plane is in parentheses.

Obviously, we can also produce random stackings either of X, Y, or Z planes using these grain boundaries, since, in each case, there are two kinds of slabs of canonical cells that could be inserted between two identicl adjacent planes. In particular, the (110) stacking fault observed in R(Al-Cu-Li) by Dubost *et al.*[82] is $A(X)BC(X)A$, where one layer of BC structure is inserted in the bcc A structure. [An X plane is a (110) plane

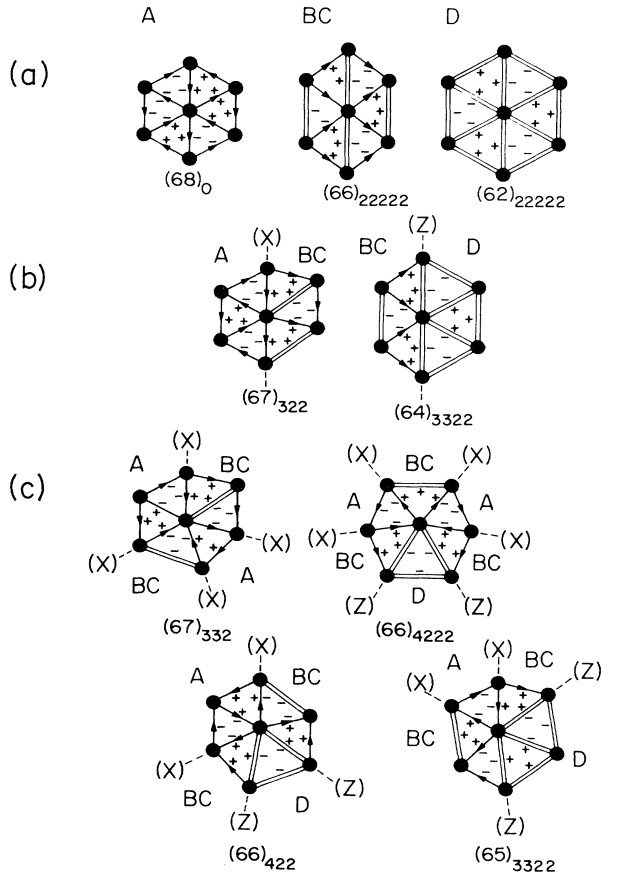

FIG. 14. Allowed nodes in *c*-stacked structures: (a) pure periodic nodes, (b) grain-boundary nodes, (c) wedge nodes. Names and possible extensions of grain boundaries and wedges are given as in Fig. 13.

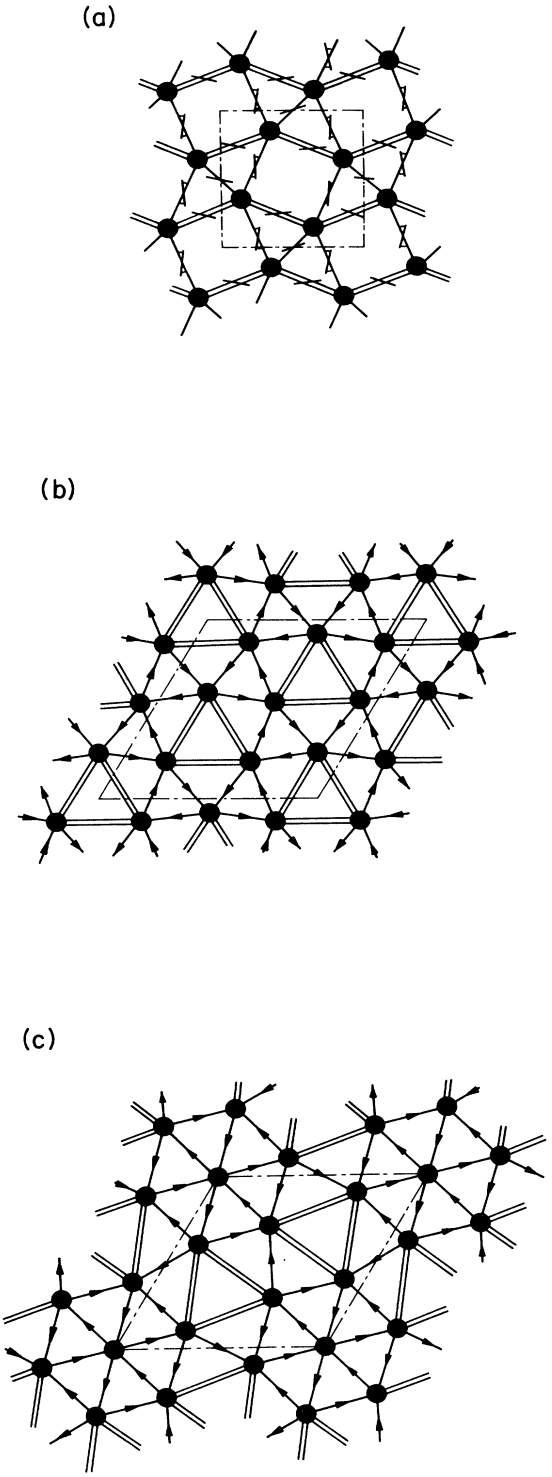

FIG. 15. Examples of periodic layered cell packings. (a) $1/1\times(2/1)^2$ orthorhombic approximant, a *b*-stacked structure; symbols are as in Figs. 10 and 12, and the unit cell is outlined with dot-dashed line. (b) 3/2-OR rhombohedral approximant. (c) a trigonal approximant. In (b) and (c) symbols are as in Figs. 11 and 13, and the *hexagonal* unit cells are outlined.

relative to the cubic axes.]

Grain-boundary intersections are lines either of *b* or *c* linkages. The structure around a line is a special case of the *b* or *c* layered structures of Sec. IV D, made by taking one of the "wedge" local environments in the bottom row of Fig. 13 or the bottom two rows of Fig. 14 (respectively). The radiating linkages are repeated along the dashed lines to form grain boundaries of the types labeled, and similarly the wedges between dashed lines are filled periodically with cells of the types labeled to form the domains. Similarly, the environments in the first rows extend to make the domains, and the "plane" environments in the second rows extend to make the grain boundaries.

V. DISCUSSION

This section (a) outlines the problems in generating infinite canonical-cell structures, (b) reviews recent developments in related cluster models, and (c) summarizes the important results of the paper.

A. Difficulties of constructing infinite structures

A very serious technical gap in the theory of canonical cells is that no mathematically sure way has been found for packing them into infinite, aperiodic structures with icosahedral symmetry, as is ultimately needed for modeling icosahedral quasicrystals. There are reasons why this is much more difficult than for a thombohedral tiling. Here I will outline five approaches; each of these has been investigated and none of them leads to a simple solution, but all appear promising for future work.

The twelvefold symmetric two-dimensional square-triangle tiling[83,84] is used as a guide to visualization (Fig. 16) since it has many analogous difficulties.[85] The triangles are roughly analogous to the A and C tetrahedra, the squares to the B_2 and D cells.

1. Projection method (quasiperiodic)

The projection method has produced networks of icosahedra[20,46,41,48] related to canonical cells in their local order but too low in packing fraction. To improve this requires adjusting the shape of the "acceptance domain" used to select vertices for projection. Since a random-growth model[28] has achieved $f=0.62$, it is rather surprising that the best packing fraction from projection is still 0.55.[20,46,47] In a rhombus tiling with twelvefold symmetry, a local pairing of 30° rhombi to produce a square with two equilateral triangles improves the packing (it corresponds to a change in the acceptance domain). For the icoshedral networks made by projection, not even the most elementary such rearrangement has yet been identified. In the square-triangle tiling, the acceptance function for a quasiperiodic structure built

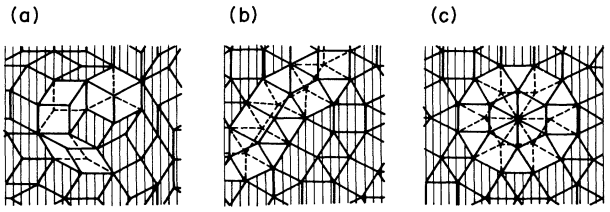

FIG. 16. Triangle-square tiling. (a) In a random rhombus tiling with twelvefold symmetry, any group of three rhombi forming a (possibly irregular) hexagon about a single vertex can be repacked (dotted lines). (b) In a triangle-square tiling, also with twelvefold symmetry, we must reshuffle an entire chain of vertices. (c) The repacking of the smallest closed chain is a 30° rotation of a dodecagon.

with Stampfli's inflation procedure[84] seems to have a fractal boundary.[86,87] The acceptance domain for a canonical-cell packing may be equally exotic; we already know that it must be disconnected if it is to have a reasonably large packing fraction.[88]

2. *Inflation rules (quasiperiodic)*

In general, inflation rules are decorations of the objects which produce another structure following the same rules but reduced by a scale factor. Now, Sec. II C showed how to decompose a canonical-cell tiling into rhombohedral units. In turn, Sec. IV C showed one way to decompose rhombohedral units into canonical cells (see Fig. 9); there are many others. The product of these two operations is a τ^3 inflation. If it permitted repeated operations, it could produce a quasiperiodic structure. (The decoration in fig. 9 cannot be repeated; it works only on the 1/1 rhombohedral tiling.) This would be analogous to Stampfli's iterative construction of quasiperiodic triangle-square tilings.[85,84,87]

3. *Monte Carlo equilibration (random tilings)*

This has been successful for random tilings, modeling entropically stabilized quasicrystal phases.[17,57,59,89,90] The fundamental move is a rearrangement of a few tiles within an otherwise unchanged geometry.[91,92] However, no simple move exists in a 2D triangle-square tiling;[85] we must rearrange an entire chain [Fig. 16(b)]. For canonical cells, the analog of the chain is probably a two-dimensional irregular slab two cells thick. We do not yet know the analog of the dodecahedron in the triangle-square tiling, i.e., a polyhedron of cell faces whose interior can be packed by cells in two different ways.

4. *Transfer-matrix iteration (random tilings)*

This approach to random tilings does not require reshufflings.[57,58,93] For canonical cells it would be based on the decomposition of (all) canonical cell tilings into well-defined layers transverse to five-fold axes (see Ref. 69 and Fig. 4.53 of Ref. 35). The method may be too ponderous for 3D tilings, since the code to generate the possible next layers would be complex and the large number of configurations drastically limits system size.

5. *Aggregation algorithms*

Growth algorithms which aggregate *nodes* carefully can produce very good packings which are almost canonical-cell packings.[28,40] Aggregations of *cells* ought to be feasible, but it is necessary to prevent generating unfillable holes on the growing surface. This is easy to do in handbuilt models since the large entropy of possible packings provides freedom to avoid bad choices. However, it may not be easy to formalize rules for the computer which work for arbitrarily large systems. (Such models would be expected to have large phason fluctuations leading to broadened diffraction peaks, similar to an "icosahedral glass."[28,29])

B. Progress in related cluster models

1. *Well-packed growth models*

The canonical objects are certainly the four best-packed polyhedra allowed in icosahedral cluster networks with b and c linkages. Thus, we naturally expect well-packed random networks to be largely composed of canonical cells. Recently, Elser has demonstrated that a growth process with annealing, using properly chosen temperature gradient and growth velocity, produces large clusters without tears.[28] He has studied the distribution of twofold and threefold bond coordination numbers (β,γ) (Ref. 28, Table I). Fully 94% of all nodes have coordinations which are allowed according to Table V (though this presumably includes some with forbidden ways of arranging the linkages around a node). Comparison of the packing fractions and average bond coordination (see Table III) also indicates that *most* of this network consists of canonical cells.

2. *Even and odd cluster models*

Any b-c cluster network can be divided without conflicts into even and odd sublattices, wherein neighbors related by c linkages have opposite parities, while those related by b linkages have the same parities. Usually the even and odd sublattices are statistically equivalent so the geometry is essentially bipartite. Fowler *et al.*[67] decorate the even nodes with large clusters, the odd ones with small clusters. This reduces the symmetry from simple icosahedral to face-centered icosahedral,[94] as seen in experiments.[95,96]

3. *Large and small cluster models*

Another type of two-cluster model has been proposed recently which is a nontrivial extension of the one-cluster geometry: a network built of both large and small fundamental clusters. Besides the same b and c linkages between any two clusters, there is a new small-small linkage of length τ^{-1} which is allowed along a twofold axis.[21,22,35,97]

This is plausible in the i(Al-Zn-Mg) class [i.e., i(Al-Cu-Li) class] of quasicrystals. Ohashi discovered[35] that the solved $Al_5Cu_6Mg_2$ structure[98] is a simple-cubic packing of small clusters connected by the short linkages; Audier speculates that Z(Al-Cu-Li-Mg) includes a triangular net of short linkages.[22] A two-cluster model was also considered in the i(Al-Mn) class by Yang,[97] who suggested generating an infinite geometry by a heirarchical rule. However, there is no evidence at present for small clusters in the icosahedral phase or related crystal phases of the i(Al-Mn) class.

Now, recall (Sec. VI A 2 above, compare Fig. 10) that decorating large (τ^3-inflated) oblate and prolate Ammann rhombohedra with cluster packings was problematic if we obey canonical-cell rules. On the other hand, with good packings of large and small clusters,[21] we can fix one highly symmetric way to decorate prolate rhombohedra, and similarly for oblate rhombohedra, consistent with any packing of the rhombohedra. This is the basis of a recent quasiperiodic decoration model for i(Al-Cu-Li) with excellent short-range order and stoichiometry.

However, these descriptions in terms of the large rhombohedra are surely incomplete. They are not sufficient to implement the matching rules that would force the infinite structure to be quasiperiodic. On the other hand, if the small and large clusters are the basic units, then (just as in the simpler networks or packings with only one cluster and two linkages) there is no reason why each large rhombohedron should be decorated identically, and moreover we can imagine many good packings that cannot be regrouped into any decoration of large rhombohedra.

It would be natural to formulate a generalized canonical-cell model by adding to the canonical set the simplest, best-packed, polyhedra with short bonds. However, this turns out to make several times as many kinds of geometrical objects as in the basic canonical-cell model presented in this paper. Since the basic model is still insufficiently understood, it may be premature to attempt its more complex versions.

C. SUMMARY

In summary, I have presented a set of geometrical rules which I present as a good basis for models of icosahedral alloy structure as well-connected packings of icosahedra. The rules (i) are based on "linkages" between clusters that are found in known crystalline alloys, and believed to predominate in the icosahedral ones, (ii) appear to have sufficient freedom to grow random structures obeying them, and (iii) are restrictive enough that the sets of cells and faces, and the possible local environments, are relatively few; among other things, such simplicity is essential if we are to construct decoration models and fit the parameters.

A language was developed in Secs. II and III to describe and compare canonical-cell packings. Section II showed how the canonical-cell packing relates to previous models built in terms of clusters or Ammann rhombohedra. Section III detailed some of the less obvious ways that canonical-cell models are simplified through restrictions on the freedom of packing (the sum rules in Sec. III A, the forcing rules for local environments in Sec. III B). It appears that taking four basic polydehra or "canonical cells" is just enough to allow icosahedral symmetry and/or extensive configurational entropy within the structure, yet few enough that many constraints are imposed (as seen in the relatively small set of possible local environments).[99] As a byproduct, we find that the canonical cells—forming simultaneously a tiling and a cluster packing— can achieve a larger packing fraction than previous models. Note that all the results of Sec. III are equally valid for random or for ideal tilings.

From Sec. III, the stoichiometry of a decoration of canonical cells can be calculated given its average phason strain and one parameter ζ characterizing the ratio of well-packed A cells and more loosely packed D cells. The frequencies of atom local environments could also be calculated given this and the frequencies of the 32 types of node local environments. It is surprising that there are so few: the number is comparable to the 24 environments in the 3D Penrose tiling,[46] but that is an *ordered, quasiperiodic* structure. The number of possible environments in an arbitrary or random tiling of the rhombohedra is 308.[100]

The packings of Sec. IV provide realistic structural models for a number of approximant crystals. Furthermore, the larger approximants serve as approximations to unbounded icosahedrally symmetric canonical-cell packings since (Sec. VI B) we still lack the rules to make them. At least Sec. IV shows that the "packing rules" of Sec. II allow a variety of structures, so that the canonical cells are a possible basis for a decoration model with random-tiling disorder. More practically, the 3/2 structural model is being used as a basis for calculations of diffraction[34] or of physical properties such as surface energy.[69,70]

It is hard to produce arbitrarily large approximants for the same reasons (Sec. V B) that it is hard to produce quasiperiodic structures. A 5/3 approximant could probably be produced starting with large rhombohedra in a 1/1 packing an decorating them by canonical cells as in Sec. V A 2; however, it seems impossible to do this with enough symmetry to make a genuinely cubic space group. In fact, each successively larger approximant required one additional kind of cell besides that in the preceding approximant (A in 1/1, BC in 2/1, D in 3/2), so perhaps a symmetric 5/3 would require yet another kind of cell.

Along the way, two different kinds of two-dimensional tilings were defined with packing rules induced by the canonical-cell packing rules: the spherical tiling of Sec. III B and the layer tilings of Sec. IV D. These have proven to be useful tools for analyzing particular canonical-cell structures.

Notes added in proof. M. Oxborrow (unpublished) has

found the analog for canonical cells of the move shown in Fig. 16. Contrary to Sec. V A 3, it forms a *chain* 2 cells in diameter. Thus, Monte Carlo is now feasible in principle for the canonical-cell tiling. A transfer-matrix calculation for a small system (Sec. V A 4) gives an entropy of 0.12 per node, much smaller than what was suggested in Ref. 17. If we modify the packing rules to disallow the nodes $(68)_0$, $(66)_{222222}$, and $(62)_{222222}$ (those of the *A*, *BC*, and *D* tilings), then $k \equiv 1$ in Eq. (3.17) and it can be shown this forces $\zeta = 0.317$ (see Sec. III A 4 and compare Tables III and VII).

ACKNOWLEDGMENTS

I am indebted to John Cahn, Howland Fowler, Jim McLean, Wataru Ohashi, and Clara Shoemaker, for useful discussions and/or comments on the draft, and particularly to Veit Elser, who first identified the canonical cells and first constructed the 3/2 cubic approximant. This work was supported by the Department of Energy through Grant No. DE-FG02-89-ER45404.

APPENDIX A: SIX-DIMENSIONAL GEOMETRY AND FREQUENCIES OF SITES

This appendix contains results of the "six-dimensional" description of quasicrystal geometry needed in this paper (Sec. III A, volume fraction of *BC* cells; Sec. IV C 1, rhombohedral cubic approximants; Sec. V A, random tilings).

1. Lift of a network to 6D and phason strain

Here I summarize needed old results and definitions. Consider a network with rigid *b* and *c* bonds, as described in Sec. II A. The linkages, and hence all internode vectors, can all be expressed (uniquely) as integer combinations of the six icosahedral basis vectors along fivefold axes $a_R \hat{e}'_i$. We select a node $\mathbf{r}_0$ arbitrarily as the origin, and then for each node position

$$\mathbf{r}^{\parallel} = a_R \sum_{i=1}^{6} n_i \hat{\mathbf{e}}_i^{\parallel} , \tag{A1}$$

we construct the perpendicular-space coordinates

$$\mathbf{h}^{\perp} \equiv a_R \sum_{i=1}^{6} n_i \hat{\mathbf{e}}_i^{\perp} , \tag{A2}$$

where we have arranged that $\hat{\mathbf{e}}_i \equiv (\hat{\mathbf{e}}_i^{\parallel} + \hat{\mathbf{e}}_i^{\perp})/\sqrt{2}$ are an orthonormal basis of a six-dimensional simple-cubic lattice.[25] If the nodes are vertices of a *tiling* in physical space, then in 6-space they define a continuous faceted three-dimensional hypersurface $\mathbf{h}^{\perp}(\mathbf{r}^{\parallel})$.

We can coarse grain our notion of $\mathbf{h}^{\perp}$ and define the *phason strain* tensor A to be the gradients of $\mathbf{h}^{\perp}$ as a function of $\mathbf{r}^{\parallel}$. That is,

$$A_{ij} \equiv dh_i^{\perp}/dr_j^{\parallel} . \tag{A3}$$

As noted below, a given set of statistical frequencies of different linkages corresponds to a unique phason strain; thus, any homogeneous structure must have a uniform phason strain.

"Random-tiling model" refers to equilibrium ensembles which (in the simplest case) are defined by giving equal weight to each different arrangement allowed by the packing rules. The number of such packings grows exponentially with system size, i.e., there is a finite entropy per site.[101] Then the statistical weighting of long-wavelength fluctuations in the tiling is expressed by the coarse-grained entropy which is a function of phason strain (defined in Appendix A). This entropy generally has a maximum at zero phason strain; this selects a state with icosahedral symmetry and (in $d=3$) Bragg peaks.[17,57–59]

2. Number ratio of rhombohedra

The object of this part is to derive the ratio (3.3) between the number densities n(PR) and n-(OR) of prolate and oblate rhombohedra, respectively. This is a generalization of the well-known relation $n(\mathrm{PR})/n(\mathrm{OR}) = \tau$ for the ideal 3DPT generated by projection,[24] to more general (possibly random) tilings with nonzero phason strain.

Consider an arbitrary tiling by the Ammann rhombohedra with an average phason strain A. We keep in mind the representation of the tiling as a faceted hypersurface. There are $\binom{6}{3} = 20$ possible orientations of 3-face in the 6D lattice which might be used as facets. These fall into two classes, ten orientations projecting to prolate rhombohedra and ten orientations projecting to oblate rhombohedra.

The number of rhombohedra of a particle orientation in the tiling is the number of corresponding 3-faces in the irregular hypersurface. This is proportional to the three-volume of the irregular hypersurface projected on the coordinate three-plane parallel to the three-face of interest. Thus, the ratio of numbers of different rhombohedra is determined by the parameters (analogous to direction cosines) which specify the average orientation of the hypersurface relative to the projection plane. For a 3-plane in 6-space, the parameters are the nine independent components of A. (An immediate corollary is that the 20 densities $n_{\alpha,\beta,\gamma}$ for different rhombohedron types are not independent, since they must depend on only nine parameters.)

Using this idea, the densities of rhombohedra for general orientation can be worked out exactly as done in Ref. 57 for two-dimensional tilings, but with *unit* basis vectors $\mathbf{e}_{(\alpha)}^{\parallel}$ in physical space and $\mathbf{e}_{(\alpha)}^{\perp}$ in perpendicular space. The result is

$$n_{\alpha\beta\gamma} = \mathbf{m}_{\alpha} \cdot \mathbf{m}_{\beta} \times \mathbf{m}_{\gamma} , \tag{A4}$$

where the vectors $\mathbf{m}_{\alpha}$ live in physical space and are given by

$$\mathbf{m}_{(\alpha)} \equiv = \tfrac{1}{2}[\hat{\mathbf{e}}_{(\alpha)}^{\perp} + (\mathbf{e}_{(\alpha)}^{\perp} \cdot \mathrm{A})] . \tag{A5}$$

In a structure with (statistical) icosahedral symmetry, A=0 so the $\{\mathbf{m}_{\alpha}\}$ are proportional to the rhombohedron edge vectors and the triple vector product (A5) is proportional to the rhombohedron volume.

More generally, to calculate either n(PR) or n(OR), we must insert (A5) into (A4) and sum over ten orientations.

In either case, the terms linear and quadratic in A sum to zero, and the cubic term simplifies, giving a total

$$n(\mathrm{PR,OR})=\tfrac{5}{4}(V^{\parallel}_{\mathrm{PR,OR}}+V^{\perp}_{\mathrm{PR,OR}}\det\mathrm{A})\ , \qquad \text{(A6)}$$

where $V^{\parallel}_{\mathrm{PR,OR}}$ and $V^{\perp}_{\mathrm{PR,OR}}$ are the volumes of rhombohedra in the respective spaces. It is well known that $V_{\mathrm{PR}}/V_{\mathrm{OR}}=\tau$ and furthermore, by a sort of duality, $V^{\perp}_{\mathrm{PR}}=V^{\parallel}_{\mathrm{OR}}$ and $V^{\perp}_{\mathrm{OR}}=V^{\parallel}_{\mathrm{PR}}$. From this follows (3.3), as was to be shown.

APPENDIX B: THE TWELVEFOLD NETWORK

1. Twelvefold sites

The *twelvefold network* was defined as a subset of vertices of the 3DPT generated by projection which have all 12 of the possible neighbors connected by edges (along fivefold directions). They are fairly uniformly distributed in space, and most of their relative displacements between neighbors are just b and c linkages. The network can be described in the projection method by a simple (triacontahedral) acceptance domain.[46]

Pairs of twelvefold sites have separation a_R; to exclude such unrealistic separations a deterministic rule is used to remove one site from each pair. The resulting (still quasiperiodic) structure is called the *twelvefold packing*. The removals cut pieces out of the acceptance domain and it becomes a complicated shape.[20,46] (Actually, there are several slightly different twelvefold packings depending on the rule we choose for deleting sites.)

The twelvefold packing was studied in detail in an earlier paper, Ref. 46; I return to it here because(1) it gives the best known *quasiperiodic* cluster packing with b and c links; studying it highlights how much better a quasiperiodic canonical cell packing would be, and (2) it contains many canonical faces and cells; hopefully it can give some suggestion of the statistics in the canonical-cell tiling (especially the parameter ζ defined in Sec. III A).

2. Frequencies of "cells" in twelvefold network

Let us determine the density of canonical-cell-shaped patterns in the twelvefold *network*. These are not cells proper: they sometimes overlap, because the short (a_R length) neighbors are not removed.

The frequency of patterns can be calculated using volumes in perpendicular space. Recall that a polyhedron of nodes corresponds to a perpendicular-space polyhedron.[46] The displacements of the latter polygon, which keep all its vertices within the acceptance domain, map out a subdomain whose volume is proportional to the frequency of the physical-space polyhedron. (Amusingly, the perpendicular-space patterns corresponding to the canonical cells happen to be the same shapes but smaller by τ^{-3}.) By Monte Carlo integration as in Ref. 46, I found about 2.15 A cells per twelvefold vertex; the D subdomain was determined exactly and analytically there are $2\tau^{-6}=0.111$ D cells per vertex. The volume ratio of A and D cells then corresponds to $\zeta=0.19$.

3. Frequencies of linkages in twelvefold packing

The average linkage coordinations in the twelvefold *network* are known to be $\bar{Z}_b=6+2\tau^{-3}$ and $\bar{Z}_c=6-2\tau^{-7}$, from Ref. 46 (Table VI and Sec. IV A). We can derive them for the twelvefold *packing* using information from that paper.

We must count the total number of linkages removed. When a node is removed, we count each linkage with a weight -1, except the weight is $\frac{1}{2}$ when the node at the other end is also removed. The only kind of environment with a close neighbor is $(175)_{5322}$, and exactly half of these are removed. It turns out that, besides the obvious neighbor by the short a_R connection, each such site also has exactly two neighbors of the same type by the b linkages near the center of the left part of Fig. 17 in Ref. 46. Assuming, for simplicity, that we choose at random which node of the short pair to remove, then each of these two b linkages counts $-\frac{3}{4}$ [the deterministic prescription for removal of Ref. 46, Fig. 9(b), would make little difference]. The fraction of removed nodes is $x=\tau^{-5}$ and each carries $5+2(\frac{3}{4})=6.5$ of the b linkages and 5 of the c linkages, so the new coordinations are

$$\bar{Z}'_b=[\bar{Z}_b-2(6.5)x]/(1-x)=5.825\ ;$$

similarly $\bar{Z}'_c=5.528$. Using Eqs. (3.9) and (3.10), a canonical-cell packing with the same ratio $\bar{Z}_c/\bar{Z}_b$ would have $\zeta=0.542$.

APPENDIX C: AUDIER-GUYOT NETWORK

1. Construction of network

Audier and Guyot[38,49] introduced a decoration of the rhombohedral 3D Penrose tiling quite different from the "twelvefold" decoration, which produces a similar network of b and c linkages. One starts with a 3DPT composed of prolate and oblate rhombohedra (PR and OR) inflated by τ^2, i.e., with edge length $A_R=\tau^2 a_R$. (Note how these are smaller than the τ^3-inflated rhombohedra seen in Figs. 9 and 10 of this paper, and also used in later models of Audier and Guyot.[21])

The even vertices of the 3D rhombohedral tiling all become even nodes of the network. Each PR also contains an interior site dividing its long diagonal in the ratio $1{:}\tau$, nearer to the even tip. All the odd nodes of the network sit on selected interior sites. To avoid close node neighbors, we must remove interior sites so that, if two PR share a face around their (common) even tip, one must be empty. This is a problem of partitioning the graph of mutually excluding sites, and an efficient heuristic algorithm was used to optimize the packing.[38,49]

2. Optimal occupation and packing fraction

All mutually excluding sites are in PR with a common even tip. Thus, the graph breaks up into disjoint finite subgraphs, each encircling an even node; manifestly, the global density is maximized if it is maximized for each subgraph. This is easy provided we started from the usual 3DPT constructed by projection.

For each of the 24 kinds of local environment in the

3DPT,[46] the possible odd sites are in those threefold directions with a sharp PR tip (a "P_1" corner in the notation of Ref. 46). For each of these, the optimal number of c linkages was found, by hand, using the pictures of the local environments of the 3D Penrose tiling.[102] Often several distinct arrangements had the same optimal number; if we choose by a deterministic rule, the result is quasiperiodic but has a face-centered icosahedral Bravais lattice (see Sec. V) since the even and odd nodes are not equivalent.

The optimal number M of associated odd nodes is summarized by the rule $M=N(P_1)$ if $N(P_1)\leq 4$; $M=N(P_1)-1$ if $N(P_1)=5$ or 6; $M=6$ for the environment $(10\,5\,0)_3$; otherwise, around twelvefold environments $(12\beta 0)_p$ we have $M=8$ for $p=0$, $M=9-p$ for $p=1,2$, and $M=10-p$ for $p=3,4$.

Knowing the frequencies of the environments (Ref. 46, Table III),[103] this gives the packing fraction

$$f_{AG}\cong 0.5584\ . \tag{C1}$$

This is better by 0.9% than that of the twelvefold packing, and therefore currently the best known packing fraction for a quasiperiodic b-c network.

APPENDIX D: ENUMERATION OF ENVIRONMENTS

Two independent methods were used to generate (by hand) a "tree" containing each local environment exactly once. A two-stage method based on linkages is described below. Both approaches found 32 distinct environments, as tabulated in Table VI.[65]

The local environment is treated as a set of linkage directions, i.e., the set of vertices of the 2D spherical tiling rather than the tiles. We count all ways to place vertices, subject to the forcing rules of Sec. III C 1. A *priori*, these conditions are necessary for an environment to be "canonical," but not sufficient, so at the end it was checked that a valid spherical tiling is formed. Remarkably, it was valid in every case, which shows that, in fact, the forcing rules $F0$–$F4$ are not only necessary but sufficient.

A quite different and less efficient method was also used based on building up the 2D spherical tiling; instead of a b-linkage arrangement, the numbers of D_a and D_a tiles contained, and how these adjoined with each other, was used for the first stage of classification. Given this, the rest was built outwards from the initial D_x tile by the rules in Fig. 5; most choices were forced.

1. First stage

We begin by identifying all ways of arranging the b linkages consistent with (a) $\beta=5$, 6, or 7 (Sec. III C 2 showed that only these values are allowable), and (b) obeying forcing rules $F3(b)$ and $F4$ (the other ones refer to c linkages). Organizing by b linkages is more efficient; if one fills in c linkages first, there is often no valid way to complete the environment with b's. To avoid generating the same configurations twice, the standard orientation for pictures of Sec. III B 2 was employed.

The first stage was subdivided into two parts. First, "maximal" b arrangements were generated: arrangements satisfying rule $F3(b)$ in which any additional b would violate the rule. Obviously all allowed b packings are part of at least one maximal packing. The maximal arrangements have $\beta=6$ or 7 while (see Table V) canonical arrangements have $\beta=5$, 6, or 7. The second part of this stage, then, is to find all arrangements obeying rules $F3(b)$ and $F(4)$ obtained by removing, at most, one [or, if $N(b)=7$, two] of the b linkages from a maximal arrangement. (Of course, some duplications must be eliminated here since many canonical arrangements can be made from more than one maximal one.)

It was found that there were only eight maximal b packings, all with the number of b links $\beta=6$ or 7. Seven of these are the b arrangements represented in environments $(76)_{433}$, $(75)_{4422}$, $(75)_{4332}$, $(75)_{3333}$, $(67)_{322}$, $(62)_{222222}$, and $(68)_0$. The eighth corresponds to a b arrangement like Fig. 17 in Ref. 46; its name would be $(7\gamma)_{5322}$, so it violates rule $F4$, but removals from it generate several legal arrangements. After the removals, 25 canonical arrangements of b's were found.

2. Placement of c linkages

The second stage, filling in with c's, turns out to be very easy. First note that each b can usefully be viewed as filling up the two triangles next to it, and the c as filling up its triangle—in fact, this is exactly the way the rhombohedra which represent these linkages take up the solid angle. (As noted in Sec. III B 1, any unfilled triangle it part of either a C_a or a D_b corner.) When two triangles of the icosahedron were left unfilled surrounded by b's, there were two choices, so one or the other must receive a c linkage. This freedom is the difference between $(66)'_{4222}$ shown in Fig. 7(b), and $(66)_{4222}$ which can be deduced from Fig. 14. It is responsible for five primed-unprimed pairs of node types in Table VI, all of them except for $(66)_{432}$ and $(66)'_{432}$.

---

*Current address.

[1]C. L. Henley, Comments Conden. Mat. Phys. **13**, 59 (1987).
[2]See the reprint collection, *The Physics of Quasicrystals*, edited by P. J. Steinhardt and S. Ostlund (World-Scientific, Singapore, 1987).
[3]P. Guyot and M. Audier, Philos. Mag. B **52**, L15 (1985).
[4]V. Elser and C. L. Henley, Phys. Rev. Lett. **55**, 2883 (1985).
[5]R. Ramachandrarao and G. V. S. Sastry, Pramana **25**, L225 (1985).
[6]C. L. Henley and V. Elser, Philos. Mag. B **53**, L59 (1986).
[7]J. W. Cahn, D. Gratias, and B. Mozer, J. Phys. (Paris) **49**, 1225 (1988).
[8]D. Gratias, J. W. Cahn, and B. Mozer, Phys. Rev. B **38**, 1638 (1988); D. Gratias, J. W. Cahn, M. Besiere, Y. Calvayrac, S. Lefebrve, A. Quivy, and B. Mozer, in *Fractals, Quasicrystals, Chaos, Knots, and Algebraic Quantum Mechanics*, edited by A. Amann, L. S. Cederbaum, and W. Gans (Kluwer Academic, Dordrecht, 1988).
[9]C. Janot, J. Pannetier, M. de Boissieu, and J. M. Dubois, Europhys. Lett. **3**, 995 (1987).

[10]C. Janot, M. de Boissieu, J. M. Dubois, and J. Pannetier, J. Phys. Conden. Mat. **1**, 1029 (1989); Chr. Janot, J. Pannetier, J. M. Dubois, and M. de Boissieu, Phys. Rev. Lett. **62**, 450 (1989).

[11]M. Audier, P. Guyot, M. de Boissieu, C. Janot, and M. V. Jarić (unpublished); M. de Boissieu, C. Janot, J. M. Dubois, M. Audier, M. Jarić and B. Dubost, in *Quasicrystals,* edited by M. V. Jaric and S. Lundqvist (World-Scientific, Singapore, 1990), p. 109.

[12]S. Y. Qiu, M. V. Jarić, C. Janot, and M. de Boissieu (unpublished); S. Y. Qiu and M. V. Jarić, in *Quasicrystals* (Ref. 11), p. 19.

[13]P. W. Stephens and A. I. Goldman, Phys. Rev. Lett. **56**, 1168 (1986); **57**, 2331 (1986).

[14]P. M. Horn, W. Malzfeldt, D. P. DiVincenzo, J. Toner, and R. Gambino, Phys. Rev. Lett. **57**, 1444 (1986).

[15]P. A. Heiney, P. A. Bancel, P. M. Horn, J. L. Jordan, S. LaPlaca, J. Angilello, and F. W. Gayle, Science **238**, 660 (1987).

[16]C. A. Guryan, A. I. Goldman, P. W. Stephens, K. Hiraga, A. P. Tsai, A. Inoue, and T. Masumoto, Phys. Rev. Lett. **62**, 2409 (1989).

[17]C. L. Henley, in *Quasicrystals and Incommensurate Structures in Condensed Matter,* edited by M. J. Yacaman, D. Romeu, V. Castaño, and A. Gómez (World-Scientific, Singapore, 1990), p. 152; M. Widom, in *Quasicrystals,* edited by M. V. Jarić and S. Lundqvist (World-Scientific, Singapore, 1990), p. 337.

[18]P. A. Bancel, Phys. Rev. Lett. **63**, 2741 (1989).

[19]C. L. Henley, in *Quasicrystals,* edited by T. Fujiwara and T. Ogawa (Springer, Berlin, 1990).

[20]M. Duneau and C. Oguey, J. Phys. (Paris) **50**, 135 (1989).

[21]M. Audier and P. Guyot (unpublished).

[22]M. Audier, Ch. Janot, M. de Boissieu, and B. Dubost, Philos. Mag. B **60**, 437 (1989).

[23]A. L. Mackay, Kristallografiya **26**, 910 (1981) [Sov. Phys.—Crystallogr. **26**, 517 (1981)].

[24]P. Kramer and R. Neri, Acta Crystallogr. A **40**, 580 (1984).

[25]V. Elser, Phys. Rev. B **32**, 4892 (1985).

[26]V. Elser, Acta Crystallogr. A **42**, 36 (1986).

[27]M. Duneau and A. Katz, Phys. Rev. Lett. **54**, 2688 (1985); A. Katz and M. Duneau, J. Phys. (Paris) **47**, 181 (1986).

[28]V. Elser, in *Aperiodic Crystals III,* edited by M. V. Jarić (Academic, New York, 1989); see also, V. Elser, in *Fractals, Quasicrystals, Chaos, Knots, and Algebraic Quantum Mechanics,* edited by A. Amann, L. S. Cederbaum, and W. Gans (Kluwer Academic, Dordrecht, 1988), pp. 121–138.

[29]P. W. Stephens, in *Aperiodic Crystals III,* edited by M. V. Jarić (Academic, New York, 1989).

[30]C. L. Henley, Physica A **140**, 306 (1986).

[31]M. Audier, P. Sainfort, and B. Dubost, Philos. Mag. B **54**, L105 (1986).

[32]Y. Shen, S. J. Poon, W. Dmowski, T. Egami, and G. J. Shiflet, Phys. Rev. Lett. **58**, 1440 (1987).

[33]D. D. Kofalt, I. A. Morrison, T. Egami, S. Preische, S. J. Poon, and P. J. Steinhardt, Phys. Rev. B **35**, 4489 (1987).

[34]C. L. Henley (unpublished).

[35]W. Ohashi, Ph. D. thesis, Harvard University, 1989.

[36]L. Levine, K. Kelton, P. Gibbons, and J. Holtzer (unpublished).

[37]M. Audier and P. Guyot, in *Quasicrystals and Incommensureate Structures in Condensed Matter,* edited by M. J. Yacamán, D. Romeu, V. Castaño, and A. Gómez (World-Scientific, Singapore, 1990), p. 288; M. Audier, P. Guyot, and Y. Brechet, Philos. Mag. Lett. **61**, 55 (1990).

[38]M. Audier and P. Guyot, Philos. Mag. B **53**, L43 (1986).

[39]A. I. Goldman and P. W. Stephens, Phys. Rev. Lett. **57**, 2770 (1986).

[40]J. L. Robertson and S. C. Moss (unpublished).

[41]J. W. Cahn and D. Gratias, J. Phys. (Paris) Colloq. **47**, C3-415 (1986).

[42]M. V. Jarić, Phys. Rev. B **34**, 4685 (1986).

[43]Occasionally a context dependent rule is needed; i.e., it depends upon the local pattern. In such cases, to formally satisfy the uniqueness, we must define the local pattern to be an additional kind of "object." The B_2 combination used in this ppaer is a simple example of such a nonprimitive object.

[44]We must relax this criterion to study substitutional disorder; the point is that the disorder should be physical, not an artifact of our ignorance.

[45]Hypothetical asymmetric decorations to implement "matching rules" (Refs. 53 and 54) are included by this criterion, since the symmetry of the geometrical objects is already reduced by the matching-rule markings.

[46]C. L. Henley, Phys. Rev. B **34**, 797 (1986).

[47]C. Oguey and M. Duneau, Europhys. Lett. **7**, 49 (1988).

[48]A. Yamamoto and K. Hiraga, Phys. Rev. B **37**, 6207 (1988).

[49]P. Guyot, M. Audier, and R. Lequette, J. Phys. (Paris) Colloq. **47**, C3-389 (1986).

[50]J. D. Bernal, Proc. R. Soc. London Ser. A **280**, 299 (1964).

[51]These four cells were originally identified by Elser (pesonal communication) as the predominant polyhedra in handbuilt models of well-packed *b-c* icosahedral cluster networks.

[52]This is reminiscent of the distinction between the actual symmetry of a space group and the symmetry (called the "holohedral group") of its Bravais lattice. However, the icosahedral group we assume here, $\bar{5}\bar{3}2/m$, *does* have inversion symmetry.

[53]J. E. S. Socolar and P. J. Steinhardt, Phys. Rev. B **34**, 617 (1986).

[54]J. E. S. Socolar, in *Quasicrystals,* edited by M. V. Jarić and S. Lundquist (World-Scientific, Singapore, 1990), p. 182.

[55]This situation is reminiscent of that for the "PLI" Penrose tiling, Ref. 53, in which the same matching rules were enfored either by decomposing the cells into the smaller cells of a deflation or else by markings on their faces.

[56]If we count X faces as we counted Y faces, we just get (3.1) again.

[57]C. L. Henley, J. Phys. A **21**, 1649 (1988).

[58]M. Widom, D. P. Deng, and C. L. Henley, Phys. Rev. Lett. **63**, 310 (1989).

[59]K. H. Strandburg, L. H. Tang, and M. V. Jarić, Phys. Rev. Lett. **63**, 314 (1989).

[60]In writing components of A, I use the convention for the basis vectors in physical and perpendicular space of M. V. Jarić, J. Phys. (Paris) Colloq. **47**, C3-82 (1986); Phys. Rev. B **37**, 4458 (1988).

[61]Y. Ma, E. A. Stern, and F. W. Gayle, Phys. Rev. Lett. **58**, 1956 (1987).

[62]Y. Ma and E. A. Stern, Phys. Rev. B **38**, 3754 (1988).

[63]C. H. Bennett, J. Appl. Phys. **43**, 2727 (1972).

[64]D. R. Nelson 1983, Phys. Rev. B **28**, 5515 (1983).

[65]See AIP document No. PAPS PRBMD-43-993-58 for 58 pages containing pictures of all 32 node environments in the canonical-cell tiling. Order by PAPS number and journal reference from American Institute of Physics, Physics Auxiliary Publication Service, 335 East 45th Street, New York, NY 10017. The price is $1.50 for each microfiche (98 pages) or $5.00 for photocopies of up to 30 pages, and $0.15 for each additional page over 30 pages. Airmail additional. Make

checks payable to the American Institute of Physics.
[66]C. L. Henley, J. Non-Cryst. Solids **75**, 91 (1985).
[67]H. A. Fowler, B. Mozer, and J. Sims, Phys. Rev. B **37**, 3906 (1988).
[68]H. Tsunetsugu, T. Fujiwara, K. Ueda, and T. Tokihiro, J. Phys. Soc. Jpn. **55**, 1420 (1986).
[69]T. Lei and C. L. Henley, Philos. Mag. B (to be published).
[70]A. J. Melmed, H. B. Elswijk, and H. A. Fowler, Philos. Mag. B **61**, 811 (1990).
[71]Note this subtlety: if we just take the set of node center positions, they form an array which often has a *higher* symmetry. To get the correct space group, we must take their decorations into account.
[72]L. Bendersky, R. J. Schaefer, F. S. Biancaniello, W. J. Boettinger, M. J. Kaufman, and D. Shechtman, Scr. Metall. **19**, 909 (1985).
[73]Thus, *any* tiling of Ammann rhombohedra with a given lattice constant must have the same numbers of OR and PR. In particular, the canonical-cell "approximants," when decomposed into Ammann rhombohedra as in Sec. II C, must contain the same numbers of OR and PR as the true approximant constructed by projection.
[74]The same set of nodes was independently constructed by Cahn and Gratias starting from the projection technique. They found it as the 3/2 approximent of a quasiperiodic structure (see Ref. 41) essentially identical to my "twelvefold packing."
[75]M. Kuriyama, G. G. Long, and L. Bendersky, Phys. Rev. Lett. **55**, 849 (1985).
[76]It has been argued by E. Prince, Acta Crystallogr. A **43**, 393 (1987), that the structural model should be based on inflated rhombohedra of this size. This decoration of the inflated rhombohedra by clusters explains (in part) why Prince's picture is a good approximation.
[77]Z. Zhang and K. H. Kuo, J. Microsc. **146**, 313 (1987).
[78]M. Audier and P. Guyot, J. Phys. (Paris) Colloq. **47**, C3-405 (1986).
[79]P. A. Bancel, P. A. Heiney, P. M. Horn, and P. J. Steinhardt, Proc. Nat. Acad. Sci. USA **86**, 8600 (1989), and references therein.
[80]K. K. Fung, X. D. Zou, and C. Y. Yang, Philos. Mag. Lett. **55**, 1 (1987).
[81]D. S. Zhou, H. Q. Ye, D. X. Li, and K. H. Kuo, Phys. Rev. Lett. **60**, 2180 (1988).
[82]B. Dubost *et al.*, J. Phys. (Paris) Colloq. **47**, C3-497 (1987).
[83]H. Kawamura, Prog. Theor. Phys. **70**, 352 (1983).
[84]P. Stampfli, Frühjahrstagung der Schweiz Phys. Gesellschaft **59**, 1263 (1986).
[85]P. W. Leung, C. L. Henley, and G. V. Chester, Phys. Rev. B **39**, 446 (1989).
[86]C. L. Henley (unpublished); D. P. DiVincenzo and D. Levine (unpublished).
[87]F. Gähler, Doctoral dissertation, Swiss Federal Institute of Technology, Zürich (ETH), 1988.
[88]A. P. Smith (unpublished).
[89]L. Tang, Phys. Rev. Lett. **64**, 2390 (1990).
[90]L. Shaw, V. Elser, and C. L. Henley, Phys. Rev. B (to be published).
[91]V. Elser, Phys. Rev. Lett. **54**, 1730 (1985).
[92]M. Widom, K. J. Strandburg, and R. H. Swendsen, Phys. Rev. Lett. **58**, 706 (1987).
[93]L. Shaw and C. L. Henley, J. Phys. A (to be published).
[94]C. L. Henley, Philos. Mag. Lett. **58**, 87 (1988).
[95]S. Ebalard and F. Spaepen, J. Mater. Res. **4**, 39 (1989).
[96]N. K. Mukhopadhyay, S. Rangganathan, and K. Chattopadhyay, Philos. Mag. Lett. **60**, 207 (1989).
[97]Q. B. Yang, Philos. Mag. B **58**, 47 (1988); Philos. Mag. Lett. **57**, 171 (1988); Philos. Mag. B **61**, 155 (1990).
[98]S. Samson, Acta. Chem. Scand. **3**, 809 (1949); see Struct. Rep. **12**, 8 (1949).
[99]I suspect, but have not shown, that structures built with only A and B/C cells cannot be completely icosahedrally symmetric.
[100]S. I. Ben-Abraham, Z. Kristallogr. **185**, 40 (1988).
[101]For ideal quasiperiodic tilings, the number of packings also diverges but only algebraically with system size. See F. Gähler, J. Phys. (Paris) Colloq. **47**, C3-115 (1986).
[102]The environments of the 3D Penrose tiling vertices, and also of the environments in the "twelvefold" network, were determined as part of the work of Ref. 46.
[103]For environment $(5\,6\,1)_4$, Table III of Ref. 46 should read $N(P_1P_3O_{10}O_7)=0\,4\,1\,1$.